Review on Solid-State-Based Marx Generators

Zhengyi Zhong, Junfeng Rao, *Senior Member, IEEE*, Haotian Liu, and L. M. Redondo, *Senior Member, IEEE*

***Abstract*— Marx generators are widely used to produce transient high-voltage pulses. The evolution of semiconductor devices and power electronics concepts promotes the development of solid-state Marx generators (SSMGs) and enables them with flexible pulse modulation ability. First, this article sorts out the evolution of SSMGs topologies chronologically. We can see that how the energy efficiency of SSMGs is considerably improved by replacing resistors with diodes and switches and how square-wave pulses are generated by SSMGs based on half-bridge structures. Unipolar and bipolar pulses can be easily produced with different SSMGs. Second, we discuss the influence of rated voltage and rated power of present semiconductor switches on the performances of SSMGs since switches are the key components in pulse generators. To reduce the size and weight of SSMGs, metal–oxide–semiconductor field-effect transistors (MOSFETs) and insulated gate bipolar transistors (IGBTs) with small packages are preferable. Third, synchronous isolated driving of switches as the crucial technique in SSMGs is introduced. Different methods of providing synchronous signals and isolated power to various stages in SSMGs are illustrated. Fourth, the performance including load capacity, droop compensation, waveform modulation, and self-triggering of SSMGs is discussed. In the end, the developing trend of SSMGs is given.**

***Index Terms*— Pulse modulation, solid-state Marx generators (SSMGs), synchronous driving, topology evolution.**

I. Introduction

THE simplest and most widely used technique to produce transient high-voltage pulses is based on the device Erwin Marx introduced, in 1925, for testing high-voltage components and equipment for the emerging power industry, the Marx generator [1]. Since then, the Marx generator has been the hinge topology for pulsed power generation and used widely from military and high-energy physics applications, where in one-shot or low repetition rate devices, hard-tube switches still dominate, to industrial high repetition rate applications, i.e., up to 100s of kHz, where semiconductor switches are used predominantly, nowadays [1]–[4].

Manuscript received July 18, 2021; revised September 15, 2021; accepted October 15, 2021. Date of publication November 3, 2021; date of current version November 18, 2021. This work was supported in part by the National Key Research and Development Program of China under Grant 2019YFC0119100. The review of this article was arranged by Senior Editor S. J. Gitomer. *(Corresponding author: Junfeng Rao.)*

Zhengyi Zhong and Junfeng Rao are with the Mechanical Engineering School, University of Shanghai for Science and Technology (USST), Shanghai 200093, China (e-mail: jfrao@usst.edu.cn).

Haotian Liu is with the Academy for Engineering and Technology, Fudan University, Shanghai 200433, China.

L. M. Redondo is with the Pulsed Power Advanced Applications Group, Instituto Superior de Engenharia de Lisboa (GIAAPP/ISEL), 1959 007 Lisbon, Portugal (e-mail: lmredondo@deea.isel.ipl.pt).

Color versions of one or more figures in this article are available at https://doi.org/10.1109/TPS.2021.3121683.

Digital Object Identifier 10.1109/TPS.2021.3121683

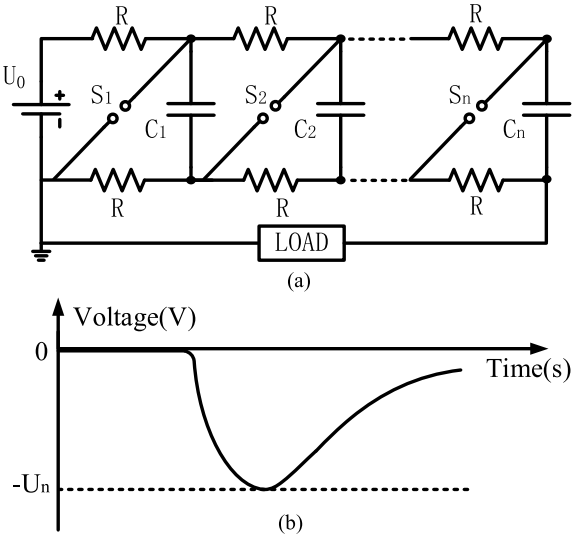

Fig. 1. (a) Classic Marx generator topology, for negative output, with n stages. (b) Exponential output voltage, into a resistive load, from circuit operation.

The aim of this article is to focus on the evolution of semiconductor, or solid-state, based Marx generators and how this evolution has been driven by power electronics concepts and the evolution of semiconductor devices. But first, in order to understand the full extension of the Marx generator technology evolution, it is necessary to know the starting point.

The Marx generator concept can be illustrated in Fig. 1, for negative output, where n energy-storing capacitors, C_i, $i \in \{1, \ldots, n\}$, are charged in parallel from a relatively low amplitude dc power supply, with voltage U_{dc}, during fairly long time, so as to the C_i capacitors achieve voltage U_{dc}. Subsequently, switches S_{pi} are turned-on, in order that all the C_i capacitors are connected in series with the load, Z_0. For the circuit in Fig. 1, the peak voltage applied to the load is, approximately, $v_0 \approx -nU_{\mathrm{dc}}$, considering no losses [1].

In Fig. 1, the classic topology, spark gaps, and resistors are used. Resistors play a double role, as they charge the capacitors during the charging mode while completing the circuit to ground, and provide a high-impedance path, forcing the current through the spark gap, during the discharge mode. The resistance values are chosen sufficiently high to limit the current through the resistors and $R \sim$ few kΩ to a few ∼MΩ is sufficient. Inductors may also be used as isolation impedances [1]. The circuit in Fig. 1 produces exponential output pulses, as shown in Fig. 1(b).

To meet the specifications for industrial applications, including higher electrical efficiency, lower capital expenditures (CAPEXs) and operating expenses (OPEXs), longer

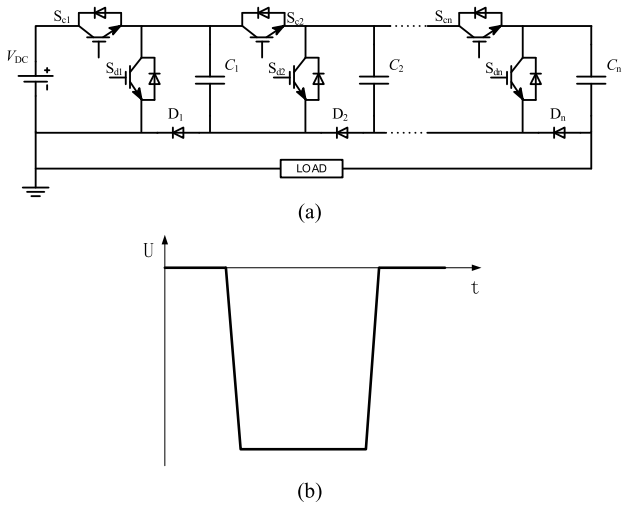

Fig. 2. (a) Modern solid-state-based Marx generator topology, for negative output, with n stages. (b) Almost square output voltage, into a resistive load, from circuit operation.

work continuity, high repetition rate, and almost rectangular output pulses, it was essential replacing the spark gaps and resistors by semiconductors, in Fig. 1 circuit. In this way, losses were limited at the same time increasing the performance of the circuit, within a reduced cost, so that nowadays it is used in many industrial and commercial applications, from tumor ablation in medical applications, ozone production in environmental applications, nonthermal pasteurization in food applications to magnetic forming in surface engineer application, with loads being resistive, capacitive, or inductive [5]–[8].

In fact, the evolution of Marx generators, specifically based on semiconductors, has been mostly dragged by commercial applications, where high repetition rate is needed, i.e., from 10s to 100 000s of Hz. This growth can be linked directly, also, to the evolution of power semiconductors manufacture, which led to the creation of a number of switching devices, with improved switching performance, being the insulated gate bipolar transistor (IGBT) and the metal–oxide–semiconductor field-effect transistor (MOSFET) the most successful.

Fig. 2 shows an example of a modern solid-state-based Marx generator, for negative output, using MOSFETs as switches. In this circuit, the S_{ci} switches and D_i diodes control the C_i capacitors charging mode and the S_{pi} switches are the pulse mode. In this case, the discharge mode was renamed pulse mode, as the C_i capacitors are only partially discharged, in order to meet the requirement for almost square-wave pulse shape for industrial applications. Fig. 2(b) shows an example of a pulse.

The renewed Marx generator in Fig. 2, using semiconductors, is now similar to a power electronic static converter topology, using common half-bridges arms, and should be designed and studied as such, with the constraint of very low duty cycle operation of the S_{pi} switches, normally $\ll 1\%$, for pulsed power operation.

Also, the performance increase can also introduce some drawbacks as the complexity of the circuit was increased, and this can affect its reliability and continuity of work, which is the first objective in industrial applications. So, in order that the circuit works with efficiency and efficacy, various aspects have to be taken care, using the techniques brought from standard power electronics converters, but also new solutions, which will be discussed in this article, as the peak power is much higher than the average power.

Hence, after this Introduction, the evolution of the solid-state Marx topologies, beginning with the introduction of diodes, only, and step-by-step going to fully solid-state replacement of all the impedances and hard-tube switches will be described in Section II, which enable the production, nowadays, of positive, negative, and bipolar output pulses for all types of loads, from resistive, to capacitive and inductive.

Then, in Section III, the type of semiconductor used to switch the voltage and currents needed for the applications, with the switching times needed, will be presented. The techniques used to send the trigger signals to the semiconductor and to supply the energy to drive them will be explained in Section IV. Also, the transition from using dedicated high-voltage modules to off-the-shelf discrete components is standard in various power electronic applications, such as the electric automotive, which are mass-produced with reduced price and lead time.

Section V aims to explain most of the methods used today for reducing the electromagnetic interference (i.e., EMI), increasing the electrical efficiency, and reducing the pulse voltage droop, multilevel operation.

Finally, in Section VI, the future trends and conclusion of solid-state Marx generator (SSMG), including smart triggering and MHz repetition rate operation will be discussed.

II. Evolution of SSMGs' Topologies

In this section, we focus on the evolution of the SSMGs' topologies where semiconductors devices are used as the main switches. In all the following topologies for SSMGs, all the main capacitors are charged either passively through resistors, inductors, or diodes or actively by charging switches. Then, these capacitors discharge to the load in series in one or two directions to generate unipolar or bipolar pulses. Since this is the common characteristics for all Marx generators, it shall not be introduced for each topology. All these topologies of SSMGs differ in the charging loops. Due to the limitation of the development of semiconductor switches, avalanche transistor has been used as the main switch of solid-state Marx circuit for a long time.

In 1966, American scientists Jung and Lewis [9] proposed an all-solid-state nanosecond Marx generator based on avalanche transistors, as shown in Fig. 3; similar to the traditional Marx generators based on spark gaps, when the avalanche transistor in the first stage is triggered ON, all other transistors breakdown automatically one by one due to the overvoltage. As a result, negative high-voltage nanosecond pulses are obtained over the load, and these pulses can be used in the treatment of biological cells [10]–[12] and the production of low-temperature plasma by array microhollow cathode discharges [13].

Many scholars adopt bipolar junction transistors (BJTs) in series and BJT Marx generators in parallel [14]–[16] to

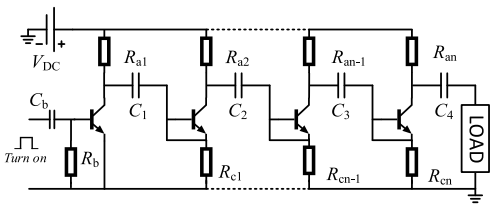

Fig. 3. Negative SSMG based on avalanche transistors.

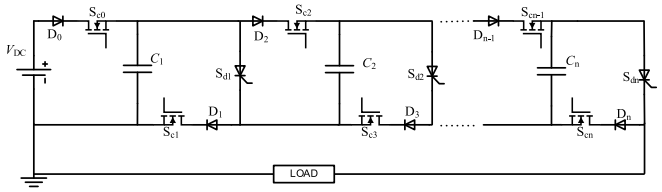

Fig. 4. Schematic of Marx generator using SCRs.

reduce the equivalent internal resistance and to improve the efficiency. Due to the low voltage and low power capacity of avalanche transistors, this type of Marx generators is not suitable for applications requiring high power pulses and long pulses. Moreover, the load capacity of these generators decreases with the increase of the number of the stages because of the equivalent ON-state resistance of the series avalanche BJTs [17]. In this topology, capacitors are still charged in parallel through resistors or inductors with high impedance and discharge to the load in series as in the classic Marx generators. Similarly, positive SSMGs based on avalanche transistors and experimental results are presented in [18]–[24]. In 1992, Grimes and Owen [25] and Jones *et al.* [26] proposed a novel topology of SSMGs based on two types of controlled devices including SCRs and MOSFETs, and the simplified schematic of which is shown in Fig. 4. SCRs are used as discharge switches, while MOSFETs serve as active recharge switches to reduce the loss in SSMGs with passive recharge and to avoid the short circuit of capacitor in each stage during discharging. Although fully controllable devices such as MOSFETs had appeared at that time, their rated power capacity was very low. Therefore, SCRs were used as the main switches due to their high-power capacity. In this topology, the high-resistance resistors in classic Marx generators were replaced by diodes in series with MOSFETs. This improvement can considerably enhance the charging efficiency. However, the widths and waveforms of pulses in this SSMG are difficult to adjust since the turning off for SCRs cannot be controlled. This presented topology with six stages was projected to reliably operate at 6-kV (15.7 A) peak voltage and at a pulse repetition rate of 15 kHz, but no experimental waveform was given in [25].

Since the 1990s, the rapid development of fully controllable semiconductor switches, such as IGBTs and MOSFETs, and the development of their drive circuits make the modulation of high-voltage pulses very flexible. IGBTs have become the most popular device in the development of SSMGs due to their good controllability and high-power capacity.

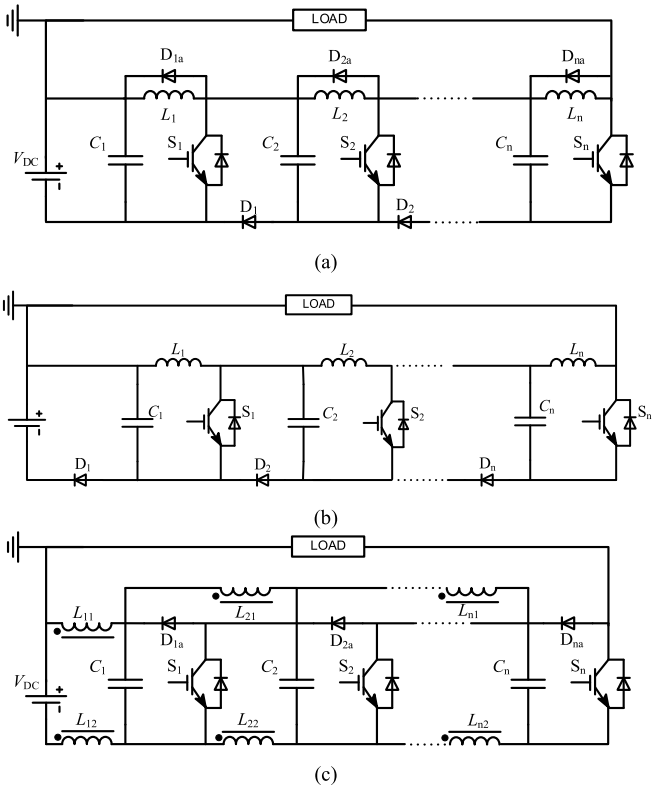

Fig. 5. SSMG with diodes and inductors in charging loops. (a) Inductors with freewheeling diodes. (b) Inductors without freewheeling diodes and (c) with chokes.

In 2000, Gaudreau *et al.* [27] from Diversified Technologies Inc. (DTI), Bedford, MA, USA, proposed an SSMG topology, as shown in Fig. 5(a), on the 24th International Power Modulator Symposium. Many diodes and inductors with diodes in parallel are used to replace the resistors and reduce the energy loss. They built a reliable prototype using 10-kV and 8-A dc power supplier, stacked IGBTs in each stage. Inductors in this SSMG topology not only limit the transient charging current but also break the short circuit of capacitors by switches such as the loop C_1–L_1–S_1 during discharging. The diodes in parallel with inductors provide freewheeling loop for the current through inductors and eliminate the induced overvoltage over the switches. Besides, all cascade inductors are in parallel with the load which makes the back edges of pulses shorter. The 500-kV and 550-A negative pulses at the frequency of 120 Hz were output to two klystrons with nominal load capacitance. The utilization of diodes and inductors in the replacement of resistors is an important step in the evolution of SSMGs because the energy loss over the resistors is avoided and the charging of capacitors is also accelerated. The quick charging also enables the high-frequency operation of SSMGs. Gaudreau *et al.* [27]–[30] from DTI made continuous contributions to the development of solid-state pulse generators. Many scholars also used the topology in Fig. 5(a) to generate high-voltage pulses with different parameters [31], [32].

In 2000, also on the same 24th International Power Modulator Symposium, Krasnykh *et al.* [33] proposed two types of SSMGs, as shown in Fig. 5(b) and Fig. 6. Compared with the

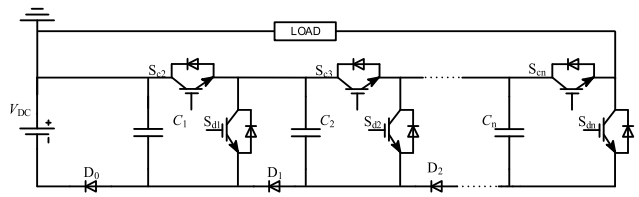

Fig. 6. SSMGs based on half-bridge structures.

topology in Fig. 5(a), the freewheeling diodes of inductors are skipped in Fig. 5(b) since both the charging and discharging current in the application of X-band TWT are much lower than that in the linear collider. A ten-cell SSMG for driving a TWT was designed and 10-kV and 1.5-A negative square pulses with a width of 4 μs at 120 Hz were obtained.

In the topology shown in Fig. 6 [33], IGBTs are used both as active recharge switches and discharge switches. There are two IGBTs in each stage, which are connected as a half-bridge circuit. The active recharge switches not only improve the charging efficiency but also provide a short circuit in parallel with the load which further shorten the back edges of pulses. Therefore, square pulses with short edges can be generated using this topology [34] though no experimental result was given in [33]. This type of half-bridge-based SSMG topology makes them very efficient and compact to flexibly generate repetitive square pulses with various parameters, though at the price of increased complexity and cost of the whole system. Based on the half-bridge structure, many subsequent topologies are proposed to obtain positive, negative, or bipolar square pulses using either negative or positive dc power supplies [34]–[42]. These half-bridge-based topologies of SSMGs are widely used today. In 2004, Cassel [35] from Stangenes Industries Company built a 30-stage SSMG prototype using this topology, and experimental result by high-voltage pulses with amplitude of 28 kV, rise time of less than 150 ns, and pulsewidth from 0.5 to 5 μs was obtained over a 1-kΩ load.

In 2002, Richter-Sand *et al.* [76] from North Star Research Company, Crystal Lake, IL, USA, proposed the SSMG topology, as shown in Fig. 5(c). A dc power supply of 1 kV is used to charge the capacitors of individual IGBT boards through a series of chokes. The choke inductors are designed to have a net current of zero while charging and to isolate individual boards during pulse erection. The winding inductance of 3.5 mH was selected to provide isolation for the maximum pulsewidth of 50 μs. They also used eight parallel IGBTs on each board to commute the current. Square pulses with voltage amplitude up to 25 kV and width of 50 μs were obtained over the 70-Ω noninductive resistor load.

In 2004, Back *et al.* [43] from Korea proposed two similar SSMG topologies shown in Fig. 7 on the 26th International Power Modulator Symposium. The position of diodes and inductors is different from that in Fig. 5(b). Either positive or negative pulses can be generated. Six IGBTs in series connection were used as one switch and auxiliary circuits were used to balance the transient voltage in the prototype. The pulse parameters generated are 20 kV, 300 A, 1 kHz, and 5 μs, and these pulses were applied to the vegetable juice

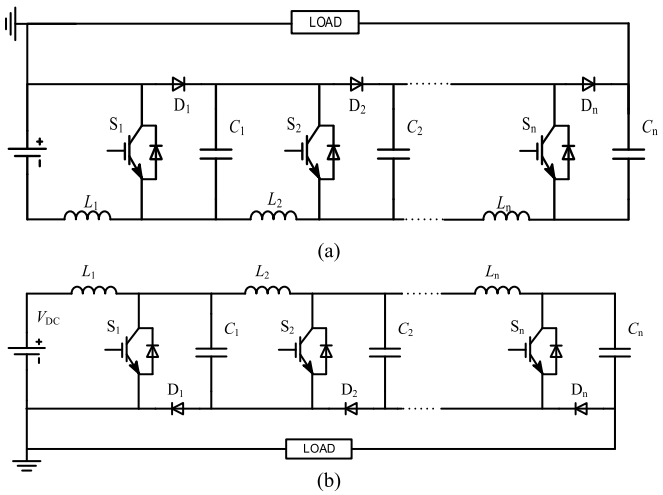

Fig. 7. SSMGs using inductors and diodes. (a) Positive SSMG with negative supplier. (b) Negative SSMG with positive supplier.

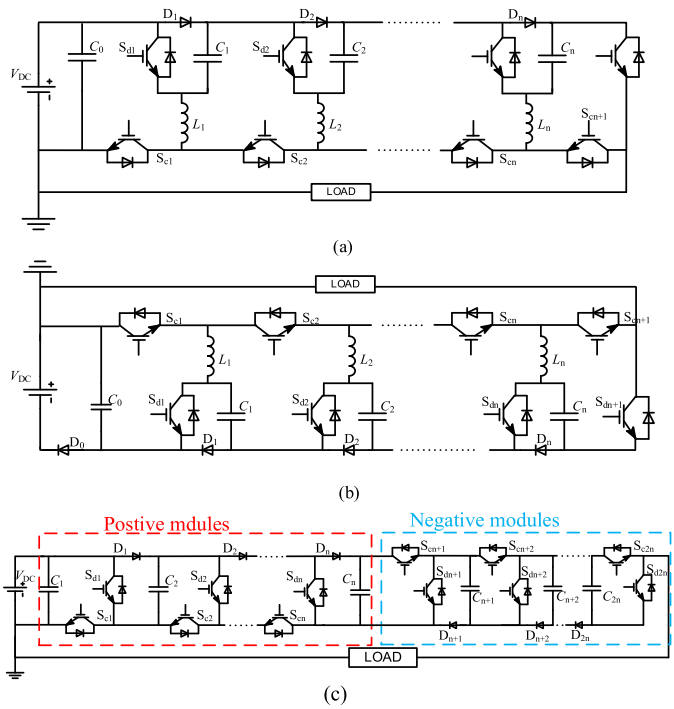

Fig. 8. (a) Positive SSMG with positive supplier. (b) Negative SSMG with negative supplier. (c) Bipolar outputs based on half-bridge structure.

for the inactivation of bacteria. The boost rate of the output voltage with discontinuous current was also investigated in this article. They proved that the output voltage is almost a multiple of the input voltage at low duty cycle. A 0.5log reduction per ten pulses was obtained.

In 2005, Cassel [38] from Stangenes Industries Company, Palo Alto, CA, USA, proposed three topologies of SSMGs, in his patent. The topology in Fig. 8(a) contains an inductor between the active recharge switch and the discharge switch in each stage. These inductors not only limit the surge current in the charging period but also can be used to adjust the rise time of pulses in the discharging period. Moreover, these inductors can also be short-circuited and then this topology becomes a

half-bridge-based SSMG similar to that in Fig. 6. This topology can generate positive square pulses. The other two are charged by positive supplier but with negative or bipolar outputs, as shown in Fig. 8(b) and (c) [35], [39], [40], [44]. The topology in Fig. 8(b) is almost the same as that in Fig. 6 except that there are more inductors L_i in each stage which helps to limit the charging surge current and modulate the rise time of pulses. The topology shown in Fig. 8(c) connects n-stage positive modules and n-stage negative modules in series to generate bipolar high-voltage pulses. To make this topology clear, the inductors have been short-circuited in Fig. 8(c). When all the active recharge switches S_{ci} (where i is between 1 and $2n$) turn on, all capacitors are charged to V_{dc} and the load is short-circuited which makes the back edges of pulses very short. When the discharge switch S_{di} in positive modules (where i is between 1 and n) and the recharge switch S_{ci} (where i is between n and $2n$) in negative modules turn on, positive pulses are generated over the load. When the discharge switch S_{di} in negative modules (where i is between n and $2n$) and the recharge switch S_{ci} (where i is between 1 and n) in positive modules turn on, negative pulses are generated over the load. The topology in Fig. 8(c) is the first publicly proposed bipolar Marx generator. In 2007, Cassel [38] was granted a relative patent in the USA and a relative patent in China granted in 2008. In these patents, the technique of droop compensation and diode strings with auxiliary power supply for driving power supply were also given.

In 2005, Portugal scholars Redono *et al.* [36], [37] also proposed two types of SSMGs based on half-bridge structures using positive dc power supplies to generate negative or positive pulses, as shown in Fig. 9. The resistor R_0 refers to the internal resistance of the dc power supply. The main difference is that they add one more switch S_{c1} in Fig. 9(a) or S_{c0} in Fig. 9(b) after the dc power supply on the basis of the topology in Fig. 8(a). In the discharging period, this switch is OFF and prevents the pulsed current flowing through the dc power supply. Therefore, the dc power supply is protected, and the reliability of the system is improved. They built a five-stage laboratory prototype using the topology in Fig. 9(a) and negative square pulses of 5-kW peak power, 10 kHz, 5 kV, 10 μs width, and 50-ns rise time were obtained over a resistive load. They were authorized a patent in Portugal in 2004. Later, they did a lot of research on the topologies of bipolar SSMGs and the influence of semiconductor switches with different materials or their combinations to increase voltage or current ratings. In 2019, Rao *et al.* [42] built a 52-stage SSMG using the topology in Fig. 9(b). High-voltage repetitive square pulses with voltage amplitude of 40 kV and width from 2.5 to 200 μs were given. It can also work at a high frequency up to 200 kHz in the burst mode.

In 2005, Dale *et al.* [45], [46] from the Los Alamos National Laboratory, Los Alamos, NM, USA, proposed the topology of SSMG using a high-voltage lumped inductor to limit the discharging current through the dc power source, as shown in Fig. 10(a). Fig. 10(a) shows the schematic of the lumped inductor-based negative SSMG using a negative dc power supply. In the charging period, the charging current flows

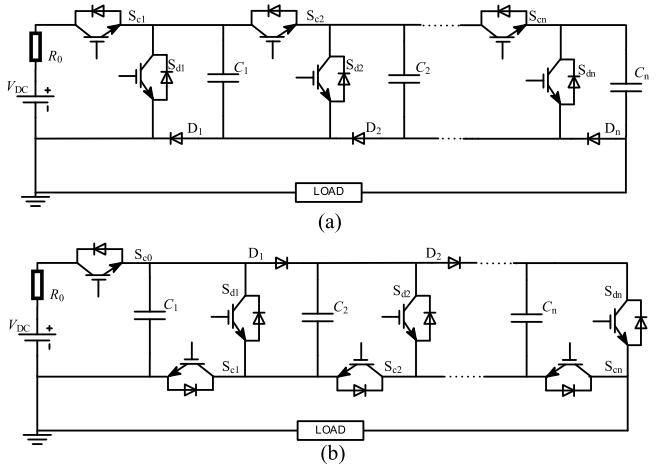

Fig. 9. Improved SSMGs based on half-bridge structure. (a) Negative output with positive supplier. (b) Positive output with positive supplier.

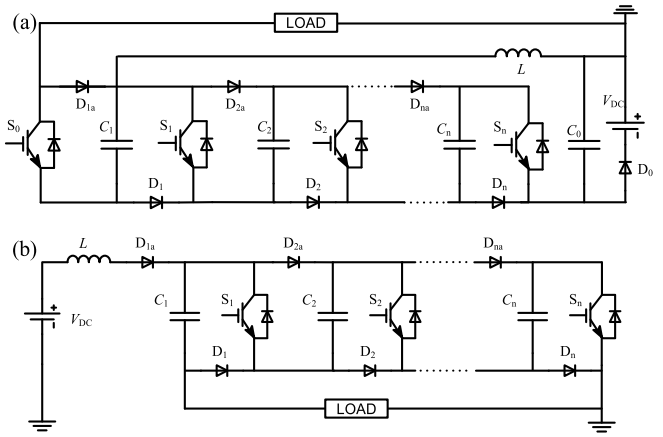

Fig. 10. Negative SSMGs using lumped inductors charged by (a) negative and (b) positive dc power supplies.

through both the inductor and diodes to charge all capacitors in parallel. In the discharging period, the high voltage generated from the series capacitors mainly discharges to the load and negative high-voltage pulses are obtained. Meanwhile, the lumped inductor limits the discharging surge current through the dc power source. Therefore, this lumped inductor should be able to withstand the pulsed high voltage and it may boost the charging voltage when the duty ratio increases [43], [47]. Since the leakage current in each stage and inter adjacent stages are blocked by the diodes rather than inductors during discharging, this topology is fit to output long pulses with higher efficiency than those in Fig. 6. The 48-stage Marx generator using this topology generated 45-kV, 165-A, 5-μs, and 50-Hz rectangular pulses to a 300-Ω test load with rise time and fall time of around 400 ns. Besides, ramp pulses, triangle pulses, and inverter triangle pulses were also obtained with dynamic control of pulse amplitudes. Fig. 10(b) shows the schematic of negative SSMGs which is charged by a positive dc power supply [48], [49]. Using this topology, Junfeng [48] built a 36-stage prototype and obtained 32-kV negative pulses over a 3.2-kΩ resistor load.

With the quick development of monopolar SSMGs and their applications in food sterilization [29], wastewater

processing [34], and bioengineering [50], bipolar SSMGs also draw some attention [51]–[61]. All bipolar SSMGs can generate positive and/or negative pulses.

In 2008, two bipolar solid-state SSMG topologies were proposed by Redondo and Silva [52] for high-voltage repetitive pulsed power applications. The schematic of the general three-stage bipolar SSMGs using six switches in each stage is shown in Fig. 11(a). There is one more capacitor than the number of stages in all topologies in Fig. 11. The general bipolar SSMG in Fig. 11(a) enables at least two redundant paths of charging the capacitors in parallel [52]. When the discharge switches S_{ai} and S_{ci} turn on, capacitors C_1, C_2, and C_3 discharge in series to the load and positive pulses are generated. When the discharge switches S_{bi} and S_{di} turn on, capacitors C_2, C_3, and C_4 discharge in series to the load and negative pulses are generated. Therefore, bipolar pulses with different widths can be generated.

The topology in Fig. 11(b) removed all the switches S_{fi} and contains five switches in each stage. In this topology, all capacitors can be only charged through one path including S_{dc}, D_{dc}, S_{ai}, D_{di}, D_i, and S_{ei}. The bipolar discharge loops are the same as that in Fig. 11(a). Using the topology in Fig. 11(b), they built a five-stage laboratory prototype which output bipolar pulses with parameters of 2 kHz, 4 kV, 15 A, and 2 μs across a resistive load. Sakamoto and Akiyama [58] also proposed a bipolar topology of SSMG using this H-bridge structure. The only difference is that the position of the switches S_{ei} is on the upside. Using the phase shift control, the proposed prototype generated $\pm$4-kV pulses with minimum pulsewidth of 300 ns. The maximum frequency was 40 kHz.

In 2012, Redondo [57] improved the bipolar SSMG topology and proposed a new topology, as shown in Fig. 11(c). In this topology, there are only four switches in each stage which makes this topology much easier and cheaper than the previous ones. However, the charge switches S_{fi} and S_{ei} have to be on either in the positive or negative discharge periods, which makes the control very complicated and deteriorates the reliability of the system. Its semiconductor's fault tolerance is also tested in [61]. Using this bipolar SSMG topology, they built a 27-stage prototype including two stages for voltage droop compensation in 2015. It generated bipolar pulses with voltage amplitude of 27 kV and current amplitude of 30 A into an 850-Ω resistive load for the industrial food processing [59].

In 2013, they further improved the four-switch bipolar topology and proposed a new one, as shown in Fig. 11(d) [62]. The adjustment is to change the positions of S_{fi} and S_{ei} so that they only function as charge switches. When the discharge switches S_{ai} turn on, capacitors C_1, C_2, and C_3 discharge in series through them to the load and positive pulses are generated. When the discharge switches S_{di} turn on, capacitors C_2, C_3, and C_4 discharge in series to the load and negative pulses are generated. In this new four-switch bipolar SSMG topology, still, only four switches in each stage are used and the control is also much easier than the previous ones. The cost and reliability of the whole system are also considerably improved.

In 2010, Bae *et al.* [53] proposed a bipolar topology by adding an H-bridge at the output of a positive SSMG for

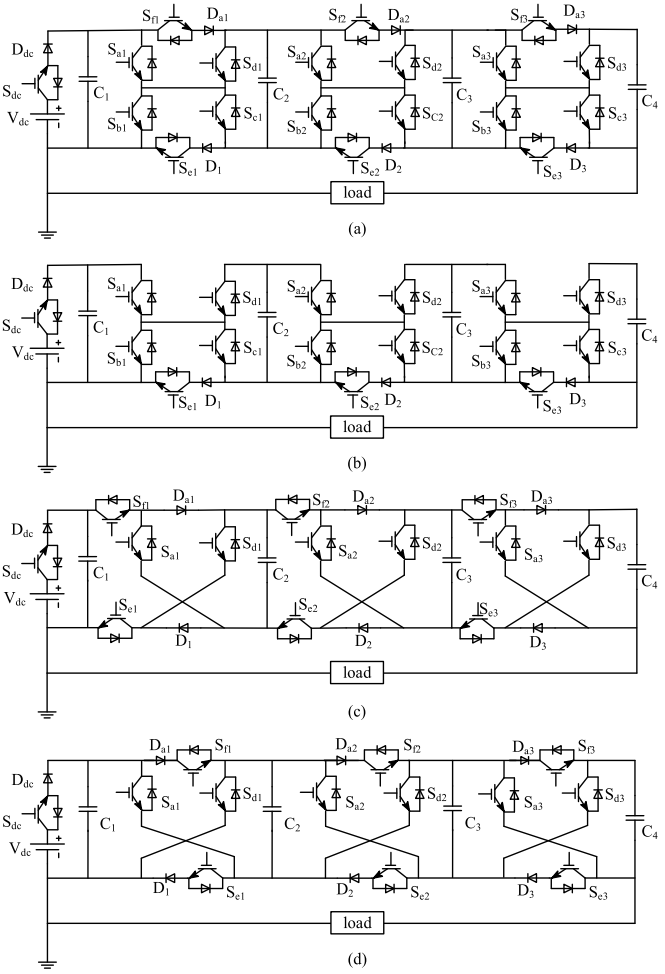

Fig. 11. Four bipolar topologies of SSMGs using different numbers of switches in each stage. (a) Six switches. (b) Five switches. (c) Four switches. (d) Improved four switches.

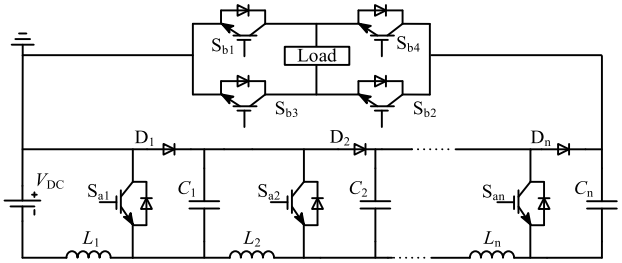

Fig. 12. Bipolar pulses by Marx generator connected to a full-bridge converter.

inversion of pulse polarities. The schematic of this topology is shown in Fig. 12. Suppose that S_{ai}, S_{b3}, and S_{b4} are all ON, positive pulses are obtained over the load. Then, negative pulses are obtained when S_{ai}, S_{b1}, and S_{b2} are all ON. The 1-kV/200-A bipolar pulses were obtained in [53]. The drawback of this structure is that output voltage amplitude is limited by the rated voltage of the switches in the H-bridge.

In 2011, based on the diode–capacitor bidirectional resonant circuit [63], Zabihi *et al.* [64] proposed a novel Marx topology in Fig. 13(a), which uses a buck–boost converter to charge the diode–capacitor units in parallel and all capacitors discharge to

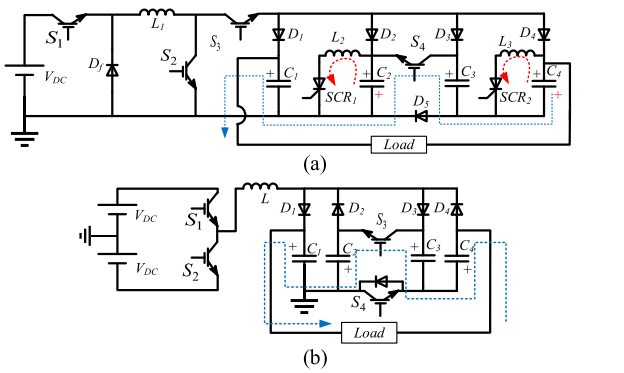

Fig. 13. Two topologies of positive SSMGs based on commutation circuits using (a) single and (b) double dc power supplies.

the load in series. When the charging period ends, the switches SCR_i turn on and the voltages over the capacitors C_{2i} reverse after half a resonant circle. Then, the switches SCR_i turn off and the switches like S_4 turn on which connect all capacitors in series to the load through the loop indicated by the blue dotted arrowed line. Almost at the same time, they proposed another one that charges the capacitors in two directions with two dc power supplies, as shown in Fig. 13(b) [64], [65]. In the discharge period, the discharge switch S_3 turns on and all capacitors are connected in series and discharge to the load in series through the loop indicated by the blue dotted arrowed line. Though both topologies generate high-voltage pulses with fewer components than other SSMGs, the rise time is very slow and pulse shapes are undesirable. Moreover, the load is always floating which is not safe.

In 2016, Yao *et al.* [60] proposed bipolar SSMGs based on two dc power supplies, as shown in Fig. 14(a). The positive power supply charges the capacitors C_{2i} to $V_{\rm dc}$ in parallel and the negative power supply charges capacitors C_{2i-1} to $-V_{\rm dc}$, through the switches S_{bi}, respectively [60]. The directions of adjacent switches S_{ai} and S_{bi} are opposite. There are 12 MOSFETs, six diodes, and seven capacitors in this three-stage SSMG. When the switches S_{a1}, S_{b2}, S_{a3}, S_{b4}, S_{a5}, and S_{b6} turn on, they connect the capacitors C_1–C_6 to the load and negative pulses are delivered to the load. When the switches S_{b1}, S_{a2}, S_{b3}, S_{a4}, S_{b5}, and S_{a6} turn on, they connect the capacitors C_2–C_7 to the load and positive pulses are delivered to the load.

In 2020, Yu [66] proposed bipolar SSMGs based on the half-bridge structure, as shown in Fig. 14(b). This topology replaces S_{ei} in the five-switch bipolar SSMG in Fig. 11(b) with inductors L_i and places them on the upper side [66]. The ten-stage prototype generated pulses with ±10-kV peak voltage, 10-kHz repetition rate, and 5-μs pulsewidth across the 500-Ω resistor load.

It should be noticed that the polarities of output pulses are mainly determined by the grounding of the loads and how the discharge switches connect capacitors in series to the loads. The pulse polarities are not limited by the polarity of the dc charging power supply. For example, positive or negative square pulses can be generated with the topology in Fig. 9(a) or in Fig. 9(b), while all capacitors are charged by a positive power supply. The topologies in Figs. 8(b) and 9(b)

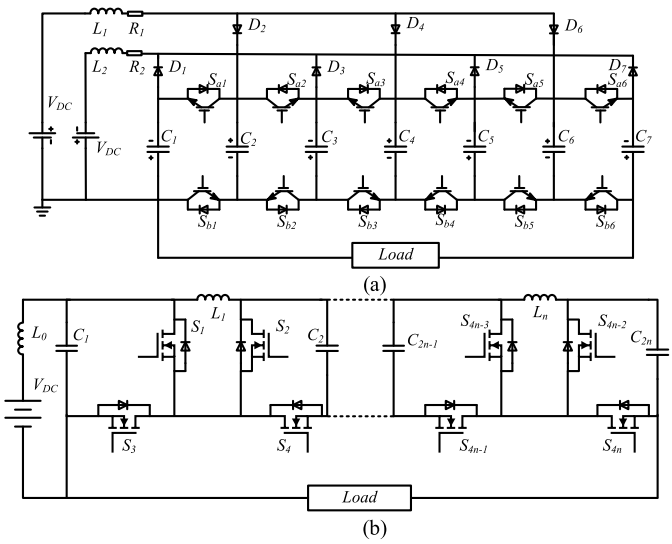

Fig. 14. (a) Three-stage dual power charging bipolar SSMG and (b) bipolar SSMGs based on half-bridge structure.

both generate negative square pulses with either negative or positive dc power supply.

Many similar topologies of solid-state pulse adders are not included in this article [67]–[72]. The main reason is that pulse adders are always charged by high-frequency resonant ac power supplies, and the capacitors are equivalently charged in series rather than in parallel.

These topologies of SSMGs are compared and summarized in the tabular form. Unipolar topologies are compared and listed in Table I and bipolar topologies in Table II.

III. Development of Semiconductors on SSMG

The progress of semiconductor switches is the main factor contributing to the evolution of Marx generators. Although there are examples of applications of almost any type of semiconductor switch ON Marx generators, for example, as seen in Section II, avalanche transistors and silicon-controlled rectifiers, the two main semiconductor switches used in solid-state-based Marx generators, from research to commercial applications, are the IGBT and the MOSFET, besides the diodes.

The main reason for this preference is not separated from the fact that these two types of power semiconductors are also at the center of many advances in the technology of power electronics associated with the railway electric traction, the renewable power generation, and electrical mobility in the last three decades, resulting in switching devices with improved switching performance, higher availability, and reduce cost.

One important aspect when choosing the type of switch to be used in the solid-state-based Marx generator is that this type of circuit, for pulsed power applications, operates with duty cycles less than 1%, which means that the peak voltage and current are much higher than the root-mean-square (r.m.s) values

In order to understand the voltage and current ratings, let us choose the circuit topology in Fig. 9(b) for monopolar

TABLE I
SUMMARY OF MARX GENERATORS WITH UNIPOLAR OUTPUTS

	Diagram of a Single Stage	Voltage Gain (n Stages) (V_{out}/V_{in})	Blocking Components between Stages	Source in Figures	Switch Type	Features
Traditional MGs	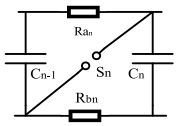	-n	Resistors	Fig. 1(a)	Spark Gaps	※High current output ※Low repetitive frequency ※Uncontrollable pulse width
Unipolar SSMGs without Charging Control (Only one switch in each stage)	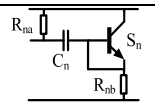	-n	Resistors	Fig. 3	BJTs	※Usage of avalanche voltage of switch ※Uncontrollable pulse width ※Low power ratings ※Nanosecond pulses
	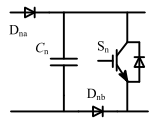	+n or -n	Diodes	Fig. 10	IGBT/ MOSFET	※Charging through the load ※Not for capacitive loads
	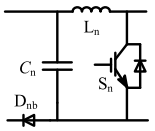	+n or -n	Inductors	Fig. 5(b) and Fig. 7	IGBT/ MOSFET	※Improved charging efficiency ※Only for narrow pulses ※Proper for resistive and capacitive loads
Unipolar SSMGs with Charging Control (Two switches in each stage)	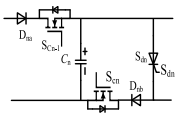	n	MOSFETs	Fig. 4	SCRs	※Redundant devices in charge loop ※Uncontrollable pulse width ※High-current capability
	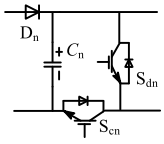	n	Diodes and Switches	Fig. 9(b)	IGBT/ MOSFET	※Classic half-bridge structure per stage ※Fast charging ※Square pulses for capacitive loads ※Shooting-through risk
	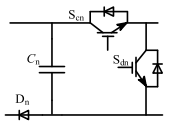	-n	Diodes and Switches	Fig. 9(a)	IGBT/ MOSFET	※Classic half-bridge structure per stage ※Fast charging ※Square pulses for capacitive loads ※Shooting-through risk
	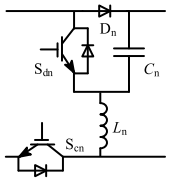	n	Diodes and Inductors	Fig. 8(a)	IGBT/ MOSFET	※Surge current limitation ※Square pulses for capacitive loads ※Low shooting-through risk
	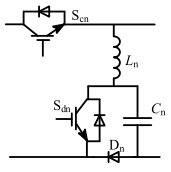	-n	Diodes and Inductors	Fig. 8(b)	IGBT/ MOSFET	※Surge current limitation ※Square pulses for capacitive loads ※Low shooting-through risk

*Different topologies require dc power supplies with different polarities and ground connection.

positive pulses and the circuit topology in Fig. 11(c) for bipolar pulses as they are some of the most used in industrial applications.

In relation to the voltage and current ratings, the Marx circuit should have voltage modularity; this means that all the components, semiconductors, and capacitors hold off the same

TABLE II
SUMMARY OF TOPOLOGIES OF BIPOLAR SSMGS

Diagram of a Single Stage	Voltage Gain (n Stages) (V_{out}/V_{in})	Number of Capacitors	Full Figure	Switches per stage	Features
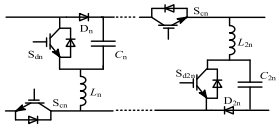	±n	2n	Fig. 8(c)	2	※Surge current limitation ※Square pulses for capacitive loads ※Low shooting-through risk ※Positive and negative modules in series
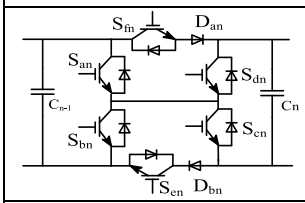	±(n − 1)	n	Fig. 11(a)	6	※Redundant switches ※Less Capacitors required
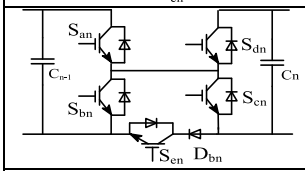	±(n − 1)	n	Fig. 11(b)	5	※Reduce voltage ratings of switches ※Less charge switches
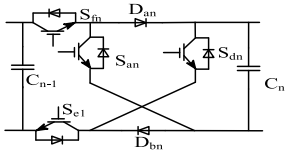	±(n − 1)	n	Fig. 11(c)	4	※Less switches and very compact ※Discharge through charging switches
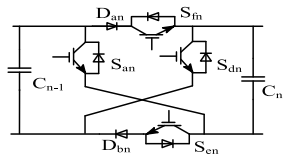	±(n − 1)	n	Fig. 11(d)	4	※Control becomes easier ※Improved reliability of the system ※Lower on-state resistance
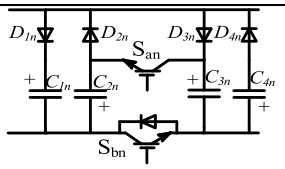	±n	4n	Fig. 13	2	※Less switches but more capacitors ※Slow rise time and undesirable pulse shapes. ※Load floating
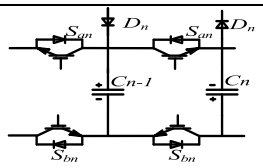	±n	n	Fig. 14(a)	4	※Two voltage power supplies ※Less capacitors
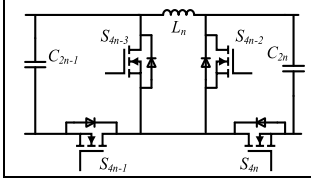	±n	2n	Fig. 14(b)	4	※Complex in control ※Only for narrow pulses ※Square pulses

voltage amplitude, which is the voltage of the input power supply V_{dc}. So the voltage rating should be at least 30% higher in order to guarantee reliability. Switches in series can be used to increase the voltage rating as in [73].

As for the current, there is no current modularity for the charging devices, in the circuit of Fig. 9(b), as the capacitors are charged in parallel; thus, the devices on the first stages hold higher current during charging. This problem can be significant depending on the output average power of the circuit, as this indicates higher charging currents and eventually higher voltage drops on the capacitors after pulse mode. Nevertheless, one should understand that SSMGs are used to apply almost square pulses, so the capacitors are normally partially discharged, only, to about 90% of their full charge. In addition, the pulse

devices carry a current, during the pulse, which is much higher in comparison with the charging devices. However, in case that some discharging switches fail to turn on during discharging, the pulse current flows through the diodes and the body diodes of charging switches, as shown in Fig. 20(a), and the diodes and the charging switches should also be able to withstand the pulse current.

In relation to the circuit of Fig. 11(c), all the semiconductor switches must carry the pulse current, where two of them are, also, used during the charging process. Also, in relation to the current rating, it is a good practice to choose switches that can carry at least 30% higher peak current.

Having said this, it is not standard to use different switches devices for charging and pulse modes, unless the difference in cost is significant.

IGBTs have been used in higher voltage and power applications, either in modules or discrete packing. IGBT modules have greater voltage ratings, being an alternative to increase the stage voltage, reducing the number of stages, as the ranges 3.3 and 4.5 kV are commercially available for different manufactures [15], [74], [75]. In addition, if the average output power is in the range of tens to 100s kW, it might be the appropriate option; otherwise, many parallel devices should be used. However, their utilization presents several drawbacks, first the price and availability (i.e., lead time). Then, normally the peak current amplitude is in the order of the dc current amplitude, which results in an oversize selection of devices. Discrete IGBT devices, such as the package TO-247, have lower power rating and voltage up to 1700 V, but peak current amplitude is much higher than the dc current amplitude, which is a good alternative for many applications, for lower power ratings, up to a few tens kW. Generators with frequencies up to a few 100s Hz, pulsewidths in the range of a few μs to 100 μs, and peak current up to 100s A [59], [76], [77] are built using discrete IGBTs. Nowadays, the TO-247-4 package has been gaining importance as it enables to reduce the gate inductance during trigger. The 1.2-kV standard has been gaining popularity due to the cost-effective and shorter lead time, because it is also one of the standers for the automotive industry.

In addition, when using IGBT modules, it is almost mandatory to use dedicated integrated trigger circuits, having the same voltage hold-off, including desaturation protection [15], [74], [75]. The problem is that these types of circuits are optimized for inductive applications, where the propagation delays of signals and protection timings are, most of the times, not compatible with pulsed power applications. Hence, it is necessary to design dedicated drive circuits with much less propagation delays and faster protection times, to be able to handle shorted pulsewidth signals and fast-rising short-circuit currents, where, for example, with resistive loads, short-circuit current goes to forbidden values in the submicrosecond range. The trigger circuits used in SSMGs are introduced in Section IV.

One of the advantages of several solid-state Marx topologies is that commercial drive circuits optimized for half-bridge power static converters can be used on Marx circuits, as, for example, the circuits in Figs. 9(b) and 11(c) can be seen as static converters that operate with stacked half-bridge semiconductor structures [15], [74], [75].

MOSFETs are the choice for repetition rates above a few kHz and pulsewidth down to 100s of ns. However, the high conduction resistance limits their application to less than 1 kV. In the last decade, a new family of SiC discrete MOSFETs begun to appear with voltage hold off up to1700 V and most important with very low conduction resistance, with increasing currents up to 100s A for pulse operation [76]. Yu *et al.* [78] compared the experimental results of the linear transformer driver (LTD) modules using silicon MOSFETs and SiC MOSFETs.

Nowadays, most of the solid-state-based Marx generators for 100s-ns pulse applications and kHz operation are assembled with SiC MOSFET devices. Also, the ease of paralleling such devices has contributed to their spread for even kA applications [79], [80], where the most popular packages are the standard TO247-3, but also the TO-263-7 for enhanced gate triggering. Also, for SiC MOSFETs, 1.2 kV is popular and increasingly the 1.7-kV rating.

In order to increase the voltage and current ratings of semiconductor switches, it is, also, typical to connect semiconductors in series and in parallel, where the main objective for connecting semiconductors in series is to reduce the number of stages, increasing the input dc voltage, and the objective of paralleling devices is to be able to carry high peak current during pulse mode [79], [80].

However, the synchronization of many switches devices increases greatly the complexity of the trigger circuit and, as consequence, reduces the circuit reliability. Also, attention has to be put in designing the trigger and control circuits of the switches, in order to avoid EMIs during pulses, which can originate erratic switching.

It is important to note that some manufacturers make available special IGBT and MOSFET devices dedicated to pulsed power applications, i.e., high voltage and peak current ratings, in TO-247-like package, which can be very advantageous for making a research generator, but are hardly used for commercial applications, due to the cost and availability [81]. Jang *et al.* [82] compared the rise time, efficiency, and reliability of the SSMGs using IGBTs and MOSFETs, respectively. They found that the one using MOSFETs prevails over the one using IGBTs in the aspects of short rise time and switching loss, while the latter dominates in reliability and turn-on loss. One can say that pulsed power is not yet an application with high components demand so it is not yet commercial sustainable for manufacturers to invest on it, making dedicated semiconductor switches.

Nevertheless, the fact that the SSMG is a topology that is based on stacking devices, the use of off-the-shelf semiconductor switches, and mass-produced for other applications is an important asset, which has contributed to the increasing success of this topology.

Another aspect that is of great importance in commercial and industrial applications is the continuity of operation and reliability of a generator. This issue is greatly connected to the circuit redundancy, during charging and pulse modes, and the type of switch fault that can happen during operation.

Considering the latter, normally the MOSFET and IGBT fail short, i.e., the trigger of power terminals is short-circuited. This type of fault is fatal for the Marx circuit topologies, as it results in capacitor short circuit. Only if the switches fail to open, or if there is some lack of synchronization during operation, it is possible to continue working, as the Marx circuit enables multilevel operation as introduced in Section V-C. In this case, the circuits with higher number of semiconductor switches, where redundancy exists, can be an advantage, as in circuit of Fig. 11(a). However, increasing the number of switches increases cost and complexity, which affect reliability.

The solution that has been adapted is the use of modular circuit assembling, where it is easy to replace damaged circuit boards. Also, nowadays, predictive maintenance can play a role in the near future, in order to determine whether the semiconductors switches are operating within their ratings and if their characteristics, such as the ON voltage, are changing, which can be a sign for derating conditions.

In conclusion, all the aspects of semiconductor switch applicability, in nowadays SSMGs, are not much different from other power static converters in power electronics applications.

IV. Synchronous Isolated Driving in SSMGs

As introduced in Section II, many discharge switches in different stages should turn on and off simultaneously to connect the capacitors in series to the load. Therefore, synchronous isolated driving of switches is the crucial technique in SSMGs. Since some stages operate at very high-voltage potential in the discharging period, the driving circuit should withstand the high pulsed voltage between the control circuit and the high-voltage power circuit. Moreover, the high-voltage pulses with high du/dt or di/dt generated by SSMGs efficiently radiate intense EMI, which induces many noises in control and driving circuits. These noises always result in the malfunction of switches and, henceforth, break the driving circuits or switches down. Then, the system fails. Therefore, the driving circuits in SSMGs should also be electromagnetic compatible, which means they can operate normally even with very intense EMI.

To sum up, the driving circuit in SSMGs must have good synchronism, good electrical insulation, and proper electromagnetic compatibility to obtain high-voltage pulses with fast front edges. In some cases, switches in different stages are triggered one by one to modulate the pulse shapes, where synchronism is not required, and they shall be introduced in Section V. The driving of power switches determines the pulsewidths, pulse shapes, frequencies, rise time, fall time, stability, and reliability of SSMGs. Therefore, the performance of SSMGs dramatically relies on the driving circuits. The synchronous driving in SSMGs always consists of synchronous signals and driving circuits. This section briefly describes the commonly used methods in SSMGs to generate synchronous isolated signals and the floating isolated power supplies to the drive circuits. At last, a typical circuit to generate synchronous isolated signals with driving power is also given.

As shown in Fig. 15(a) and (b), optic fibers and magnetic transformers are widely used to isolate signals. Optical signals converted from electric signals transmit in optic fibers. Then, these optical signals are converted into electric signals in optic receivers. Optic isolation has many advantages including strong compatibility against interference, high isolation voltages, long-distance transmission, and wide ranges of transmission bandwidth [83]. These advantages make optic fibers effective and preferential in SSMGs. However, the cost of optic transmission is high. Optic coupling chips are cost-effective with limited isolation ratings. Transformers with their primary windings in series, as shown in Fig. 15(b), easily generate synchronous signals on their secondary windings when the current flows through the common primary winding. This is the typical synchronous signal generation using magnetic isolation. Compared with optic isolation, magnetic isolation is much cheaper. However, the width of signals is limited by the saturation of magnet cores. As a result, it cannot be used for long pulses.

To reduce the switching losses and to realize fast switching, high-speed gate drivers which can source and sink peak currents up to a few amperes are essential in solid-state pulse generators. Since all switches are at different high-voltage potentials during discharge, gate drive circuits with galvanic isolation are required to float the power supply to triggering stages [84]. Widely used methods of providing isolated power are listed as follows.

The first method is the magnetic isolated power supplies, as shown in Fig. 15(a). High-frequency ac power flows through the primary windings of many transformers and is rectified into isolated dc power and stored in capacitors [85]. Then, a dc–dc converter in each stage regulates the dc power into stable dc voltage as power supply to the drive circuit. In this way, the transformers withstand the high voltage between the primary and secondary circuits. All the driving power comes from the primary circuit at the price of increased complexity of the whole system [84].

The second type is using auxiliary capacitors to provide isolated power supplies, as shown in Fig. 16. Since the dc voltages over auxiliary capacitors C_{an} may vary in different stages, a dc–dc converter is necessary in each stage to transform them into stabilized and isolated dc voltages. The difference between the circuits in Fig. 16 lies in the source of the power in auxiliary capacitors. In Fig. 16(a), the power comes from an auxiliary dc power supply with the auxiliary diode string circuit [86]. When the charging switches from S_{c1} to S_{cn} are all ON, the auxiliary power supply charges the auxiliary capacitors through the diode string circuit [38], [39]. Though the voltage amplitudes become lower in stages far away from the auxiliary power supply, dc–dc converters with a wide range of input voltage turn them into stable dc voltages and supply power to drivers. In capacitive power supply, as shown in Fig. 16(b), autonomous auxiliary capacitors C_{ai} obtain power during the charging of main capacitors C_n since they are in series. The diodes nearby guarantee that no discharging current flows through auxiliary capacitors C_{an} [87]. In self-generating power circuit, as shown in Fig. 16(c), auxiliary capacitors fetch power from the main capacitors through R–C–D circuits

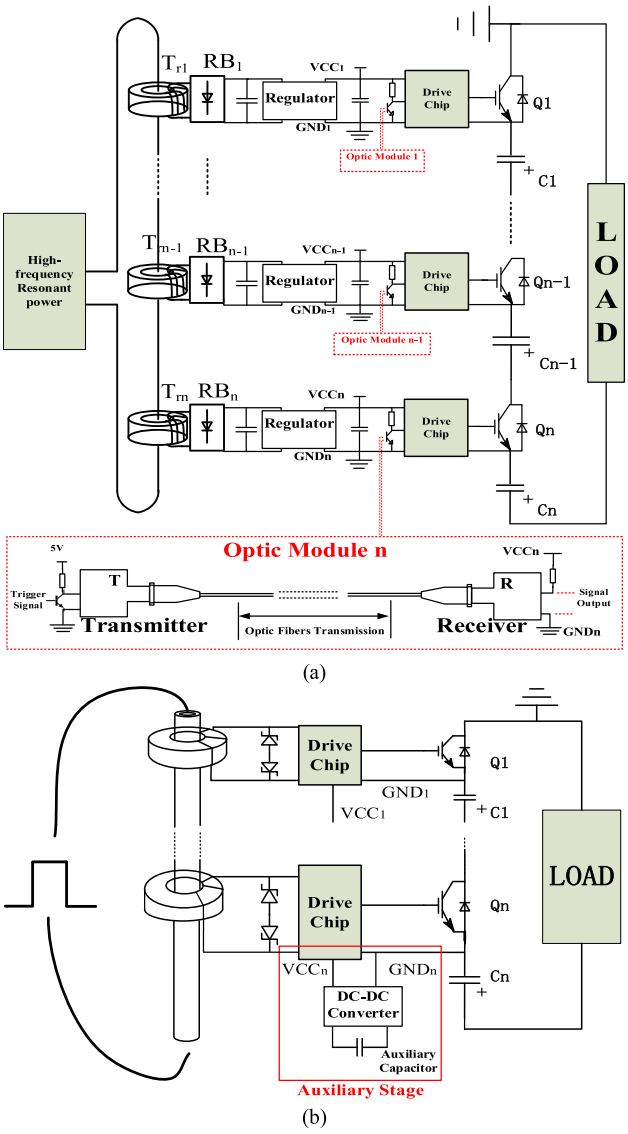

Fig. 15. Trigger signal in high insulation with (a) optic fibers and (b) magnet transmission.

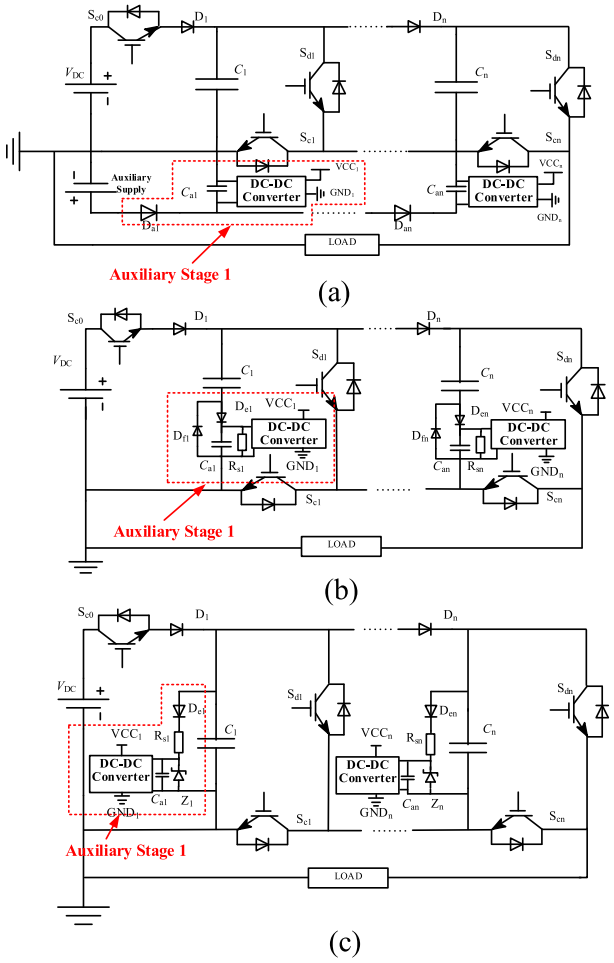

Fig. 16. Isolated power supply with auxiliary capacitor by (a) diode bootstrap, (b) autonomous capacitive power, and (c) self-generating power.

where the resistors must withstand the dc high voltages over the main capacitors.

In the above methods, commercial drivers with powerful protection and fault diagnosis functions can be used since isolated floating dc power supplies are available in all stages. Therefore, the compatibility and reliability can also be improved. However, the system becomes very complicated and the efficiency also decreases.

Transformers are usually used to deliver either signals, as shown in Fig. 17(a), or ac power, as shown in Fig. 15(a), to the secondary sides. However, the saturation of magnetic cores in transformers limits the pulsewidth of signals and only narrow pulse can be transmitted through transformers [33], [88]. A novel method of providing synchronous isolated driving based on transformers is to combine signals and driving power together. This idea was first proposed by Barnes *et al.* [89] in 1994. As shown in Fig. 17(b), bipolar pulses are input to the primary windings in series. Two FETs are used at the secondary side of each transformer. When a positive turn-on driving signal arrives, the FET S_{1-2} automatically turns on, then through D_{1-1} and S_{1-2}, the gate capacitor C_{q1} is charged to a positive high level and the switch Q1 turns on. When the positive turn-on driving signal ends, S_{1-2} automatically turns off. Since both FETs are OFF, the charges in C_{q1} leak very slowly and it can stay in a positive high level for a few milliseconds. Therefore, Q1 remains on even though the turn-on signal ends. Until a negative turn-off driving signal arrives, the FET S_{1-1} automatically turns on, C_{q1} is charged to a negative high level, and the switch Q1 turns off. When the turn-off signal ends, the negative bias voltage remains and Q1 holds on until the arrival of the next turn-on signal. As can be seen, there is no isolated power supply in the secondary circuits. Both the signals and driving power come from the bipolar pulses in the primary side which can be generated from a half-bridge [88]–[90] or full-bridge [91] circuit. High-voltage isolation and good synchronization can be easily achieved in this circuit [25]. Since the ON-state pulsewidth is determined by the time interval between the positive turn-on signals and negative turn-off signals, the magnetic saturation has no limitation on pulsewidths and negative bias gate voltage further enhances the electromagnetic compatibility of the system. Scholars from the Korea Electrotechnology Research Institute, Changwon, South Korea, also proposed some synchronous

drive circuits which provide both gate power and signal from high-voltage one-turn primary windings [91]–[94]. Besides, overcurrent protection can also be realized in these novel circuits [95].

V. Performance of SSMGs

A. Load Capacity

Due to the limited rating power of semiconductor switches, SSMGs are used to generate repetitive high-voltage pulses with peak power from 104 to 109 W. These repetitive pulses are widely used in radar modulators, linear colliders, plasma implantation, pollution control, electroporation, food processing, and so on.

In all applications, the loads can be divided into capacitive, resistive, or inductive loads. Different loads have different requirements on the switching speeds, repetitive frequencies, peak currents, waveforms, and equivalent capacitances of pulse generators.

Typical capacitive loads include dielectric barrier discharges (DBDs) which are widely used as low-temperature plasma sources [96], [97]. In DBDs loads, currents mainly appear at the rising and falling periods and the current amplitudes are proportional to the du/dt of edges. Thus, the pulsewidths have little influence on the average power of SSMGs and the average current is quite low. The equivalent main capacitance of SSMGs can be low. Moreover, repetitive high-voltage pulses with short rising and falling edges can excite more intense plasma. Besides, due to the influence of the remanent charges in DBD reactors, rectangular pulses or bipolar pulses are preferred to improve the efficiency [98], [99].

The typical resistive applications of SSMGs include electroporation and discharges in waters [79]. In these cases, the waveforms of output voltage and current are the same and the current amplitudes are proportional to the voltage over the resistive load. With resistive loads, the high discharge currents and long pulse duration easily result in severe voltage drop. Therefore, the equivalent capacitance of SSMGs should be large enough. When operating at high repetitive frequencies, the rated current and power capacity of discharging switches in SSMGs should be high enough to ensure a long lifetime. The charging speed for capacitors should also be high enough to maintain stable high-voltage amplitudes.

Purely inductive loads are uncommon in pulsed power applications, but resistive and inductive loads are very common. To reduce the cost and volume, pulsed transformers are connected at the output of SSMGs to further step up the pulsed voltage. In these cases, the loads can be always regarded as inductive [100]–[103]. The oscillations and the transient voltage over switches should be clamped. Sometimes, energy recovery and impedance matching should also be considered. The advantages and limitations of monopolar and bipolar SSMGs are discussed in [86] and [104].

B. Droop Compensation

When SSMGs generate long pulses, the voltage drops gradually during each pulse as the charges stored in capacitors are released continuously to the load. The higher is the discharging current, the more quickly the voltage drops. The simple way to eliminate the voltage droop is to increase the capacitance of SSMGs at the sacrifice of the cost, weight, and size of the pulse generators. Therefore, the idea of droop compensation comes up. The basic principle of droop compensation is that some additional stages or modules are added in SSMGs and their output are added to the load at proper moments to compensate the voltage droop dynamically during the pulse.

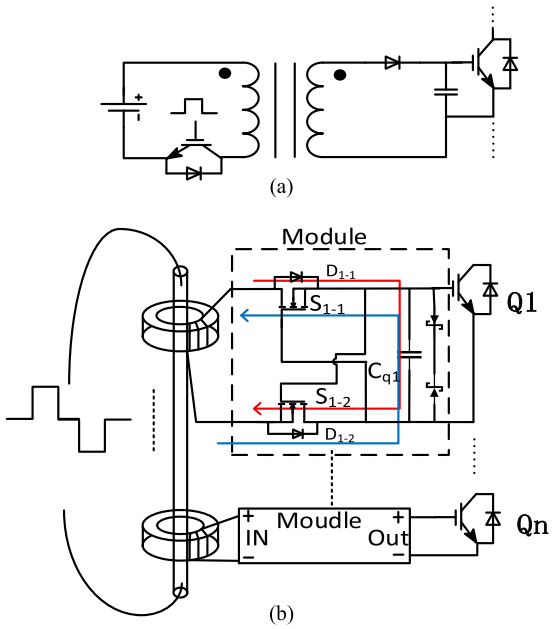

Fig. 17. Trigger signal without power supply in (a) traditional mode and (b) improved drive circuit with negative bias.

In the design of pulse generators, the capacitance of energy storage capacitors is mainly determined by the voltage amplitude, the load impedance, and the maximum pulsewidth and allowed voltage drop rate [105]. But if the droop compensation technology is used, the capacitance may be further reduced.

In 2007, Leyh [106] from the Stanford Linear Accelerator Center (SLAC) National Accelerator Laboratory, Menlo Park, CA, USA, proposed an SSMG for International Linear Collider (ILC), which operates at 120 kV, 140 A, 1400 μs, and 5 Hz on a 150-kW load. This SSMG employs 16 12-kV "main" cells and one 12-kV "vernier" regulator module, consisting of 16 internally arranged 900-V Marx cells used for fine regulation of the output pulse. In normal operation, 14 of the 16 main cells are active, with two cells parked as spares [106]. In order to produce the full 1400-μs pulselength, two cells are delay-fired at regular intervals during the pulse, producing a coarse-leveled pulsewith a 12-kV sawtooth on top of the 120-kV waveform. The equivalent circuit is shown in Fig. 18(a). When the voltage droop reaches 12 kV, the 13th cell is triggered, and the output voltage is raised to 120 kV again. When the voltage droop reaches 12 kV for the second time, the 14th cell is triggered, and the output voltage is raised to 120 kV again. The resulting sawtooth waveform after compensation is shown in Fig. 18(b). The 12-kV vernier cell further smoothes out the coarse effects to level the output pulse. Fine regulation of $\pm 0.5\%$ was realized in 2009 [107].

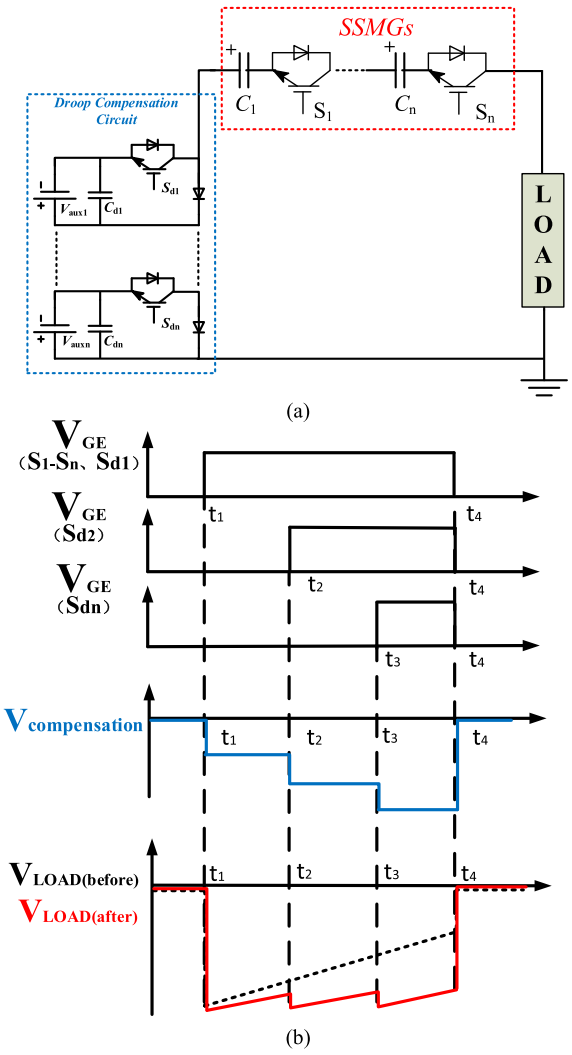

Fig. 18. Negative droop compensation circuit of SLAC with (a) diagram and (b) time sequence of control signals.

In 2008, Cassel [108] from Stangenes Industrial proposed another technique to provide smooth and flexible pulse voltage droop compensation in the existing monopolar SSMGs. An L–C filter in parallel with one stage, with no need of auxiliary power supply, operates as a buck regulator to reduce the ripple voltage [108]. This scheme of droop compensation can also be used in bipolar SSMGs, as shown in Fig. 11.

In 2016, Canacsinh [109] added resonant stages in normal bipolar SSMGs. These two auxiliary independent resonant stages are inserted into the SSMG, as shown in Fig. 19. When the switch S_r turns on, resonant oscillation occurs between C_r and L_r. Then, the linear part of the voltage over the capacitor C_r is added to the load as positive or negative droop compensation. Experimental results with 50-Hz, 4-kV, 100-μs bipolar pulses and 10% droop compensation and dynamic analysis were also given in [105] and [109]–[113].

C. Waveform Modulation

Different applications have different requirements on the waveforms of pulses. Therefore, the waveform modulation

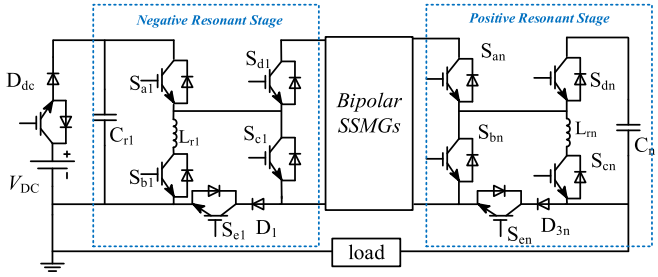

Fig. 19. Droop compensation circuit with auxiliary stages for bipolar outputs.

is very important in SSMGs. In traditional pulsed power systems using gaseous switches, the modulation of pulsewidth is difficult due to the poor controllability of gaseous switches. The modulation of waveforms of high-voltage pulses is much more challenging. On the contrary, with the wonderful controllability of semiconductor switches, SSMGs can easily generate rectangular pulses with various pulsewidths, repetitive frequency, rising/falling edges, and even waveforms. In this section, we mainly talk about multilevel modulation and pulse sharpening of SSMGs.

1) Multilevel Modulation: Multilevel generators can flexibly generate high-voltage pulses with many levels. In pulsed atmospheric discharges, the impedance of the load usually varies dynamically with the discharge voltage and current. Therefore, multilevel modulation can be used to control the waveform in these applications to obtain stable impedance and special discharge characteristics.

In normal operations, all discharge switches in an SSMG turn on and off synchronously and the voltage amplitude is proportional to the number of stages. If the discharge switches in some stages fail to turn on, the voltage amplitude decreases accordingly. Fig. 20(a) shows the classical SSMG composed of many half-bridge submodules and each switch can be triggered independently. Suppose that S_{d2} remains OFF, while all other discharge switches are ON during the discharging period, the discharge current would be bypassed through the body diode of S_{c2} and D_3. Two paths of the discharging current are indicated by the green arrowed lines. Then, the voltage amplitude of the output pulse decreases from nV_{dc} to $(n-1)V_{dc}$. In this case, the voltage over the switch S_{d2} is still V_{dc} and no overvoltage occurs. This is the voltage clamping effect in SSMGs. This effect enables SSMGs to generate multilevel pulses if the discharge switches are triggered ON and OFF one by one, as shown in Fig. 20(b). In 2011, Encarnao *et al.* [114] used this technology in Marx derived generator. In 2014, to adjust high-voltage pulse levels more flexibly, Rocha *et al.* [75], [115] proposed a circuit structure named modular Marx multilevel converter diode (M3CD) cell. When the capacitors in multilevel converter are charged by the high-frequency ac in combination with rectifiers as in pulse adders [116], [117], they have more advantages such as simple structure and flexible control. The modulator test for load transient analysis is given in [118]. In 2016, Elgenedy *et al.* [119] applied the multilevel pulses in different applications such as wastewater treatment and electroporation [120], [121].

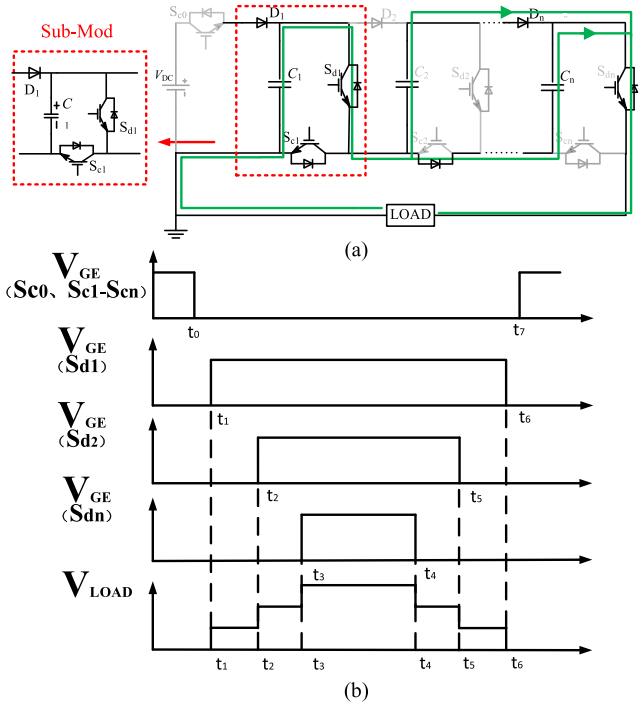

Fig. 20. M3CD structure. (a) Circuit diagram. (b) Control sequence.

When the steps in multilevel are short enough, and with enough levels, high-voltage pulses with adjustable rising/falling edges can be generated. The influence of stray capacitance is discussed in [122]. The Miller effect of switching can also be used to generate pulses with different adjustable smooth rise/fall edges [123]–[125].

2) Sharpening Circuit: Though pulses with adjustable rising/falling edges can be generated when SSMGs operate as multilevel converters, the edges are not shorter than that in normal synchronous operation. In other words, the edges can only be longer, rather than shorter. To further shorten the front edges of pulses in SSMGs, sharpening circuit should be used, especially in high current applications [126] and with high inductance in the discharging loop [127].

The sharpening circuit is shown in Fig. 21. A magnetic switch (MS) and a peak capacitor C_p are used to sharpen the rise time. The SSMG discharges to C_p first and little current flows through the load due to the high inductance of the unsaturated MS [128]. When the MS saturates, C_p discharges to the load through the saturated inductance of MS which is much lower than the total inductance of L_0. As a result, the rise time of high-voltage pulses is much shorter than that without the sharpening circuit. Magnetic pulse compression technology is widely used in pulsed power systems with resistive load [126], [128]–[131].

D. Self-Triggering

Usually, each switch in SSMGs needs a driver and there are many drivers in SSMGs. Let alone the requirements of synchronous isolated driving. The self-triggering circuits provide signals to only one switch, namely, Q1, and all other switches turn on or off automatically with the turning on and

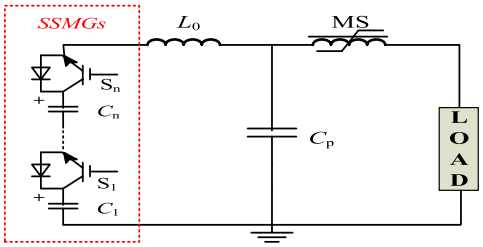

Fig. 21. Sharpening circuit diagram.

turning off of Q1 due to special auxiliary circuits [132], [133]. Therefore, self-triggering circuits make the SSMGs much simpler in structure and more compact than common driving circuits. However, the drawbacks of self-triggering circuits are also obvious. The self-triggered pulsewidths in various stages are different, and the switching speeds also become slower. Besides, the range of adjustable pulsewidths is limited [134]. Therefore, the application of self-triggering circuits in SSMGs still has a long way to go.

VI. Conclusion and Prospect of SSMGs

The Marx generator is a pulsed power technique that has been used for generating high-voltage pulses over, almost, 100 years, maintaining its basic operating principle, but at the same time incorporating the advances of the technology, so that it can be considered, nowadays, a key valuable tool in almost all the application fields.

Through this article, it was described how the evolution of the semiconductor switching technology was incorporated in the Marx generator, creating a number of circuits, based on only solid-state switches, which enable the generation of positive and/or negative pulses to different types of loads. In fact, it was shown that modern Marx-type circuits include, generally, diodes, MOSFETs, or IGBTs, based, normally, on Si or SiC technology, capable of generating ns–ms width pulses, with repetition rates up to MHz, peak currents up to kA, and peak voltage up to tens kV, originating peak power in the order of tens of MW with tens kW average powers.

In addition, as Marx generators become solid-state-based generator, all the techniques brought from power electronics were incorporated, so in this article, various triggering and protection circuits, voltage droop and waveform modulation procedures, and EMI reduction and efficiency increasing were described.

In the future, the all-solid-state Marx circuit will be further developed: 1) how to use fewer signals to drive switches and ensure their synchronicity to generate high-voltage square-wave pulses and 2) high frequency up to MHz and miniaturization and smart control and detect technology of circuit. Wide range of adjustable repetition frequency even from 0.1 Hz to MHz [135], [136], modularization, compactness and portability, smart control with user's interface [137], [138], fault detective and overcurrent protection [139], [140], switches in stacked [141] and parallel [79] to increase its voltage ratings and current ratings, or Marx in series or parallel [142], [143] are the hotspot in present and future.

REFERENCES

[1] W. J. Carey and J. R. Mayes, "Marx generator design and performance," in *Proc. Conf. Rec. 25th Int. Power Modulator Symp., High-Voltage Workshop*, Jun. 2003, pp. 625–628.

[2] W. Jiang and K. Yatsui, "Compact pulsed power generators for industrial applications," *IEEJ Trans. Fundam. Mater.*, vol. 124, no. 6, pp. 451–455, 2004.

[3] F. O. A. Jeffrey A. Casey, "Solid-state Marx bank modulator for the next linear collider," in *Proc. Conf. Rec. 26th Int. Power Modulator Symp., High-Voltage Workshop.*, Jun. 2005, pp. 641–644.

[4] J. Lehr and P. Ron, "Marx generators and Marx-like circuits," in *Foundations of Pulsed Power Technology*. IEEE, 2018, pp. 1–62, doi: 10.1002/9781118886502.ch1.

[5] M. P. J. Gaudreau, J. Casey, T. Hawkey, J. M. Mulvaney, and M. A. Kempkes, "Solid-state pulsed power systems," in *Proc. Conf. Rec. 23rd Int. Power Modulator Symp.*, Jun. 1998, pp. 160–163.

[6] S. A. Ghani, W. I. Ibrahim, M. R. Ghazali, and N. A. Azli, "Power electronics converter with Marx generator configuration based PEF for liquid food sterilization," in *Proc. Int. Conf. Electr., Control Comput. Eng. (InECCE)*, Jun. 2011, pp. 416–419.

[7] T. Huiskamp, J. J. van Oorschot, M. T. Pereira, and L. M. Redondo, "Ozone generation with a flexible solid-state Marx generator," in *Proc. IEEE Int. Power Modulator High Voltage Conf. (IPMHVC)*, Jun. 2018, pp. 147–150.

[8] L. M. Redondo, M. Zahyka, and A. Kandratsyeu, "Solid-state generation of high-frequency burst of bipolar pulses for medical applications," *IEEE Trans. Plasma Sci.*, vol. 47, no. 8, pp. 4091–4095, Aug. 2019.

[9] E. A. Jung and R. N. Lewis, "A solid state nanosecond pulser using Marx bank techniques," *Nucl. Instrum. Methods*, vol. 44, no. 2, pp. 224–228, Oct. 1966.

[10] J. R. Mayes, W. J. Carey, W. C. Nunnally, and L. Altgilbers, "The Marx generator as an ultra wideband source," in *Pulsed Power Plasma Sci. 28th IEEE Int. Conf. Plasma Sci. 13th IEEE Int. Pulsed Power Conf. Dig. Papers (PPPS)*, Jun. 2001, pp. 1665–1668.

[11] C. Yamada, T. Ueno, T. Namihira, T. Sakugawa, S. Katsuki, and H. Akiyama, "Evaluation of BJTs as closing switch of miniaturized Marx generator," in *Proc. 16th IEEE Int. Pulsed Power Conf.*, Jun. 2007, pp. 468–471.

[12] W. Ren, H. Wang, and R. Liu, "High power variable nanosecond differential pulses generator design for GPR system," in *Proc. 13th Internarional Conf. Ground Penetrating Radar*, Jun. 2010, pp. 1–5.

[13] C. Zhang and K. Q. L. Jian, "Array microhollow cathode (MHC) discharges with pretrigger device triggered by nanosecond pulses at atmospheric pressure," *IEEE Trans. Plasma Sci.*, vol. 44, no. 10, pp. 1961–1970, Oct. 2016.

[14] Z. Li, P. Li, J. Rao, S. Jiang, and T. Sakugawa, "Theoretical analysis and improvement on pulse generator using BJTs as switches," *IEEE Trans. Plasma Sci.*, vol. 44, no. 10, pp. 2053–2059, Oct. 2016.

[15] C. Li *et al.*, "Design and development of a compact all-solid-state high-frequency picosecond-pulse generator," *IEEE Trans. Plasma Sci.*, vol. 46, no. 10, pp. 3249–3256, Oct. 2018.

[16] J. Rao, W. Zhang, S. Jiang, and Z. Li, "Nanosecond pulse generator based on cascaded avalanche transistors and Marx circuits," *IEEE Trans. Dielectr. Electr. Insul.*, vol. 26, no. 2, pp. 374–380, Apr. 2019.

[17] W. Ding, Y. Wang, C. Fan, Y. Gou, Z. Xu, and L. Yang, "A subnanosecond jitter trigger generator utilizing trigatron switch and avalanche transistor circuit," *IEEE Trans. Plasma Sci.*, vol. 43, no. 4, pp. 1054–1062, Apr. 2015.

[18] S. J. Davis, "High performance avalanche transistor switchout for external pulse selection at 1.06 microm," *Appl. Opt.*, vol. 17, no. 19, pp. 3184–3186, 1978.

[19] R. J. Baker, "High voltage pulse generation using current mode second breakdown in a bipolar junction transistor," *Rev. Sci. Instrum.*, vol. 62, no. 4, pp. 1031–1036, Apr. 1991.

[20] A. Chatterjee, K. Mallik, and S. M. Oak, "The principle of operation of the avalanche transistor-based Marx bank circuit: A new perspective," *Rev. Sci. Instrum.*, vol. 69, no. 5, pp. 2166–2170, May 1998.

[21] K. Mallik, "Nonuniform doping of the collector in avalanche transistors to improve the performance of Marx bank circuits," *Rev. Sci. Instrum.*, vol. 71, no. 4, pp. 1853–1861, Apr. 2000.

[22] G. Duan, S. N. Vainshtein, and J. T. Kostamovaara, "Lateral current confinement determines silicon avalanche transistor operation in short-pulsing mode," *IEEE Trans. Electron Devices*, vol. 55, no. 5, pp. 1229–1236, May 2008.

[23] Y.-L. Guo, N.-N. Yan, S.-H. Guo, and G. Zeng, "500 ps/1 kV pulse generator based on avalanche transistor Marx circuit," in *Proc. Int. Workshop Microw. Millim. Wave Circuits Syst. Technol.*, Oct. 2013, pp. 296–299.

[24] G. Duan, S. N. Vainshtein, J. T. Kostamovaara, V. E. Zemlyakov, and V. I. Egorkin, "3-D properties of the switching transient in a high-speed avalanche transistor require optimal chip design," *IEEE Trans. Electron Devices*, vol. 61, no. 3, pp. 716–721, Mar. 2014.

[25] M. D. Grimes and T. E. Owen, "A high-repetition rate, solid-state, Marx-bank pulse generator for geophysical instrumentation," in *Proc. 20th Conf. Rec. Power Modulator Symp.*, Jun. 1992, p. 181.

[26] W. J. Sarjeant and R. E. Dollinger, "High power electronics," in *Tab Books*, 1st ed. Mar. 1989.

[27] M. P. J. Gaudreau, J. A. Casey, J. M. Mulvaney, and M. A. Kempkes, "Modulator development for the next generation linear collider," in *Proc. Conf. Rec. 24th Int. Power Modulator Symp.*, Jun. 2000, pp. 153–156.

[28] M. P. J. Gaudreau, J. A. Casey, J. M. Mulvaney, and M. A. Kempkes, "Solid state radar modulators," in *Proc. Conf. Rec. 24th Int. Power Modulator Symp.*, Jun. 2000, pp. 196–199.

[29] M. P. J. Gaudreau, T. Hawkey, J. Petry, and M. A. Kempkes, "A solid state pulsed power system for food processing," in *Pulsed Power Plasma Sci. 28th IEEE Int. Conf. Plasma Sci. 13th IEEE Int. Pulsed Power Conf. Dig. Papers (PPPS)*, Jun. 2001, pp. 1174–1177.

[30] M. Gaudreau, T. Hawkey, J. Petry, and M. Kempkes, "Solid-state power systems for pulsed electric field (PEF) processing," in *Proc. IEEE Pulsed Power Conf.*, Jun. 2005, pp. 1278–1281.

[31] K. Liu, Y. Wu, and J. Qiu, "All-solid-state pulsed power supply based on Marx generator," in *Proc. IEEE 34th Int. Conf. Plasma Sci. (ICOPS)*, Jun. 2007, p. 493.

[32] Y. Wu, K. Liu, J. Qiu, X. Liu, and H. Xiao, "Repetitive and high voltage Marx generator using solid-state devices," *IEEE Trans. Dielectr. Electr. Insul.*, vol. 14, no. 4, pp. 937–940, Aug. 2007.

[33] A. Krasnykh, R. Akre, S. Gold, and R. Koontz, "A solid state Marx type modulator for driving a TWT," in *Proc. Conf. Rec. 24th Int. Power Modulator Symp.*, Jun. 2000, pp. 209–211.

[34] J. Rao, Y. Lei, S. Jiang, Z. Li, and J. F. Kolb, "All solid-state rectangular sub-microsecond pulse generator for water treatment application," *IEEE Trans. Plasma Sci.*, vol. 46, no. 10, pp. 3359–3363, Oct. 2018.

[35] R. L. Cassel, "A solid state high voltage pulse modulator which is compact and without oil or a pulse transformer," in *Proc. Conf. Rec. 26h Int. Power Modulator Symp., High-Voltage Workshop.*, May 2004, pp. 72–74.

[36] L. M. Redondo, J. F. Silva, P. Tavares, and E. Margato, "All silicon Marx-bank topology for high-voltage, high-frequency rectangular pulses," in *Proc. IEEE 36th Power Electron. Spec. Conf.*, Jun. 2005, pp. 1170–1174.

[37] L. M. Redondo, J. F. Silva, P. Tavares, and E. Margato, "High-voltage high-frequency Marx-bank type pulse generator using integrated power semiconductor half-bridges," in *Proc. Eur. Conf. Power Electron. Appl.*, Sep. 2005, p. 8.

[38] R. L. Cassel, "An all solid state pulsed Marx type modulator for magnetrons and klystrons," in *Proc. Pulsed Power Conf.*, Jun. 2007, pp. 836–838.

[39] R. L. Cassel, R. N. Hitchcock, and S. S. Hitchcock, "A high power dynamically flexible pulse width radar modulator," in *Proc. IEEE Int. Conf. Plasma Sci.*, Jun. 2007, pp. 1492–1494.

[40] R. L. Cassel, "High voltage pulsed power supply using solid state switches," U.S. Patent 7 301 250, May 4, 2004.

[41] M. Nguyen, T. Beukers, C. Burkhart, R. Larsen, J. Olsen, and T. Tang, "Development status of the ILC Marx modulator," in *Proc. IEEE Int. Power Modulators High-Voltage Conf.*, May 2008, pp. 120–123.

[42] J. Rao, "All solid state high-frequency and high voltage pulsed power supply," *High Power Laser Part. Beams*, vol. 31, no. 3, 2019, Art. no. 035001.

[43] J. W. Baek, D. W. Yoo, G. H. Rim, and J.-S. Lai, "Solid state Marx generator using series-connected IGBTs," *IEEE Trans. Plasma Sci.*, vol. 33, no. 4, pp. 1198–1204, Aug. 2005.

[44] R. Cassel, "The evolution of pulsed modulators from the Marx generator to the solid state Marx modulator and beyond," in *Proc. IEEE Int. Power Modulator High Voltage Conf. (IPMHVC)*, Jun. 2012, pp. 9–13.

[45] G. E. Dale *et al.*, "Design and application of a diode-directed solid-state Marx modulator," in *Proc. IEEE Pulsed Power Conf.*, Jun. 2005, pp. 1211–1214.

[46] G. E. Dale *et al.*, "Performance of a diode-directed solid-state Marx modulator," in *Proc. IEEE Pulsed Power Conf.*, Jun. 2005, pp. 1033–1036.

[47] W. DongDong, *Research on Characteristics of High Power Solid-State Switch in Pulse Power Application*. Shanghai, China: Fudan Univ., 2011.

[48] R. Junfeng, *Pulse Modulation Technology of Repetitive Frequency Pulse Power Source Based on Solid State Switch and its Application*. Shanghai, China: Fudan Univ., 2013.

[49] J. Rao, K. Liu, and J. Qiu, "A novel all solid-state sub-microsecond pulse generator for dielectric barrier discharges," *IEEE Trans. Plasma Sci.*, vol. 41, no. 3, pp. 564–569, Mar. 2013.

[50] K. H. Schoenbach, S. Katsuki, R. H. Stark, E. S. Buescher, and S. J. Beebe, "Bioelectrics-new applications for pulsed power technology," *IEEE Trans. Plasma Sci.*, vol. 30, no. 1, pp. 293–300, Feb. 2002.

[51] R. Zhang, L. Wang, Y. Wu, Z. Guan, and Z. Jia, "Bacterial decontamination of water by bipolar pulsed discharge in a gas–liquid–solid three-phase discharge reactor," *IEEE Trans. Plasma Sci.*, vol. 34, no. 4, pp. 1370–1374, Aug. 2006.

[52] H. Canacsinh, L. M. Redondo, and J. F. Silva, "New solid-state Marx topology for bipolar repetitive high-voltage pulses," in *Proc. IEEE Power Electron. Spec. Conf.*, Jun. 2008, pp. 791–795.

[53] S. Bae, A. Kwasinski, M. M. Flynn, and R. E. Hebner, "High-power pulse generator with flexible output pattern," *IEEE Trans. Power Electron.*, vol. 25, no. 7, pp. 1675–1684, Jul. 2010.

[54] H. Canacsinh, L. M. Redondo, F. F. Silva, and E. Schamiloglu, "Modeling of a solid-state Marx generator with parasitic capacitances for optimization studies," in *Proc. IEEE Pulsed Power Conf.*, Jun. 2011, pp. 1422–1427.

[55] T. Sakamoto, A. Nami, M. Akiyama, and H. Akiyama, "A repetitive solid state Marx-type pulsed power generator using multistage switch-capacitor cells," *IEEE Trans. Plasma Sci.*, vol. 40, no. 10, pp. 2316–2321, Oct. 2012.

[56] L. M. Redondo and H. Canacsinh, "Bipolar solid state arbitrary-waveform Marx generator for capacitive loads," in *Proc. IEEE Pulsed Power Conf.*, Jun. 2011, pp. 598–601.

[57] H. Canacsinh, L. M. Redondo, and J. F. Silva, "Marx-type solid-state bipolar modulator topologies: Performance comparison," *IEEE Trans. Plasma Sci.*, vol. 40, no. 10, pp. 2603–2610, Oct. 2012.

[58] T. Sakamoto and H. Akiyama, "Solid-state dual Marx generator with a short pulsewidth," *IEEE Trans. Plasma Sci.*, vol. 41, no. 10, pp. 2649–2653, Aug. 2013.

[59] L. M. Redondo and M. T. Pereira, "25 kV bipolar solid-state Marx generator for industrial food applications," in *Proc. IEEE Pulsed Power Conf. (PPC)*, May 2015, pp. 1–4.

[60] C. Yao, "A novel configuration of modular bipolar pulse generator topology based on Marx generator with double power charging," *IEEE Trans. Plasma Science*, vol. 44, no. 10, pp. 1–7, Mar. 2016.

[61] W. Shin, J. Choi, and T. Kim, "Bidirectional pulse plasma power supply for treatment of air pollution," in *Proc. 37th IEEE Power Electron. Spec. Conf.*, Jun. 2017, pp. 1–6.

[62] L. M. Redondo, "New four-switches bipolar solid-state Marx generator," in *Proc. 19th IEEE Pulsed Power Conf. (PPC)*, Jun. 2013, pp. 1–5.

[63] S. Zabihi, F. Zare, G. Ledwich, and A. Ghosh, "A bidirectional two-leg resonant converter for high voltage pulsed power applications," in *Proc. IET Eur. Conf. Eur. Pulsed Power Incorporating CERN Klystron Modulator Workshop*, Sep. 2009, pp. 1–4.

[64] S. Zabihi, F. Zare, G. Ledwich, A. Ghosh, and H. Akiyama, "A new family of Marx generators based on commutation circuits," *IEEE Trans. Dielectr. Electr. Insul.*, vol. 18, no. 4, pp. 1181–1188, Aug. 2011.

[65] S. Zabihi and Z. F. Z. Zare, "A solid state Marx generator with a novel configuration," in *Proc. 19th Iranian Conf. Elect. Eng.*, May 2011, pp. 1–6.

[66] W. Zeng, "A novel high frequency bipolar pulsed power generator for biological applications," *IEEE Trans. Power Electron.*, vol. 35, no. 12, pp. 12861–12870, Dec. 2020.

[67] K. Liu, Y. Luo, and J. Qiu, "A repetitive high voltage pulse adder based on solid state switches," *IEEE Trans. Dielectr. Electr. Insul.*, vol. 16, no. 4, pp. 1076–1080, Aug. 2009.

[68] L. Gao, "All solid-state Marx modulator with bipolar high-voltage fast narrow pulses output," *IEEE Trans. Dielectr. Electr. Insul.*, vol. 18, no. 3, pp. 775–782, Jul. 2011.

[69] L. Li, K. Liu, and J. Qiu, "Repetitive high voltage rectangular waveform pulse adder for pulsed discharge of capacitive load," *IEEE Trans. Dielectr. Electr. Insul.*, vol. 20, no. 4, pp. 1218–1223, Aug. 2013.

[70] Y. Lu, K. Liu, J. Qiu, L. Li, and Y. Wang, "A solid-state bipolar pulse adder based on phase-shifted control," in *Proc. 19th IEEE Pulsed Power Conf. (PPC)*, Jun. 2013, pp. 1–4.

[71] Y. Lu, Y. Wang, J. Qiu, and K. Liu, "The design of a compact bipolar pulse current generator based on solid-state Marx adder," in *Proc. IEEE Int. Power Modulator High Voltage Conf. (IPMHVC)*, Jun. 2014, pp. 652–655.

[72] S. Jiang, J. Ge, J. Rao, and Z. Li, "Development of an all solid state bipolar rectangular pulse adder," *IEEE Trans. Plasma Sci.*, vol. 46, no. 7, pp. 2605–2611, Jul. 2018.

[73] J.-H. Kim, M.-H. Ryu, B.-D. Min, and G.-H. Rim, "200KV pulse power supply implementation," in *Proc. Eur. Conf. Power Electron. Appl.*, Sep. 2007, pp. 1–5.

[74] L. M. Redondo, F. H. M. Cavalcante, H. Canacsinh, M. T. Pereira, M. R. Gomes, and M. R. Silva, "Solid-state Marx type modulator for plasma based ion implantation applications," in *Proc. IEEE Pulsed Power Conf.*, Jun. 2011, pp. 1326–1329.

[75] L. L. Rocha, J. F. Silva, and L. M. Redondo, "Multilevel high-voltage pulse generation based on a new modular solid-state switch," *IEEE Trans. Plasma Sci.*, vol. 42, no. 10, pp. 2956–2961, Oct. 2014.

[76] R. J. Richter-Sand, R. J. Adler, R. Finch, and B. Ashcraft, "Marx-stacked IGBT modulators for high voltage, high power applications," in *Proc. Conf. Rec. 25h Int. Power Modulator Symp., High-Voltage Workshop.*, Jun. 2002, pp. 390–393.

[77] K. Liu, J. Qiu, Y. Wu, X. Liu, and H. Xiao, "An all solid-state pulsed power generator based on Marx generator," in *Proc. 16th IEEE Int. Pulsed Power Conf.*, Jun. 2007, pp. 720–723.

[78] F. Yu, T. Sugai, A. Tokuchi, and W. Jiang, "Development of solid-state LTD module using silicon carbide MOSFETs," *IEEE Trans. Plasma Sci.*, vol. 47, no. 11, pp. 5037–5041, Nov. 2019.

[79] L. M. Redondo, A. Kandratsyeu, and M. J. Barnes, "Marx generator prototype for kicker magnets based on SiC MOSFETs," *IEEE Trans. Plasma Sci.*, vol. 46, no. 10, pp. 3334–3339, Oct. 2018.

[80] M. J. Barnes *et al.*, "Future circular collider injection and extraction kicker topologies and solid state generators," *Phys. Rev. Accel. Beams*, vol. 22, Jul. 2019, Art. no. 071001.

[81] W. Jiang *et al.*, "Compact pulsed power and its industrial applications," in *Proc. IEEE Pulsed Power Conf.*, Jun. 2009, pp. 1–10.

[82] S.-R. Jang, H.-J. Ryoo, G. Goussev, and G. H. Rim, "Comparative study of MOSFET and IGBT for high repetitive pulsed power modulators," *IEEE Trans. Plasma Sci.*, vol. 40, no. 10, pp. 2561–2568, Oct. 2012.

[83] Z. Li, H. Liu, J. Rao, and S. Jiang, "Gate driving circuit for the all solid-state rectangular Marx generator," *IEEE Trans. Plasma Sci.*, vol. 47, no. 8, pp. 4058–4063, Jul. 2019.

[84] L. M. Redondo *et al.*, "Solid-state Marx type circuit for the ISOLDE voltage target modulator," in *Proc. IET Eur. Conf. Eur. Pulsed Power Incorporating CERN Klystron Modulator Workshop*, 2009, p. 27.

[85] S.-R. Jang, C.-H. Yu, and H.-J. Ryoo, "Trapezoidal approximation of LCC resonant converter and design of a multistage capacitor charger for a solid-state Marx modulator," *IEEE Trans. Power Electron.*, vol. 33, no. 5, pp. 3816–3825, May 2018.

[86] L. M. Redondo and J. F. Silva, "Repetitive high-voltage solid-state Marx modulator design for various load conditions," *IEEE Trans. Plasma Sci.*, vol. 37, no. 8, pp. 1632–1637, Aug. 2009.

[87] H. Canacsinh, L. M. Redondo, and J. F. Silva, "Isolated autonomous capacitive power supplies to trigger floating semiconductors in a Marx generator," in *Proc. IEEE Int. Symp. Ind. Electron.*, Jun. 2007, pp. 821–826.

[88] Z. Zhou, Z. Li, J. Rao, S. Jiang, and T. Sakugawa, "A high-performance drive circuit for all solid-state Marx generator," *IEEE Trans. Plasma Sci.*, vol. 44, no. 11, pp. 2779–2784, Nov. 2016.

[89] M. J. Barnes, G. D. Wait, and C. B. Figley, "A FET based frequency and duty factor agile 6 kV pulse generator," in *Proc. 25t Int. Power Modulator Symp., Conf.*, Jun. 2002, pp. 1–4.

[90] M. J. Barnes and G. D. Wait, "A FET based kicker for a charge booster for the TRIUMF ISAC project," in *Proc. IEEE Conf. Rec. Abstracts. PPPS- Pulsed Power Plasma Sci. 28th IEEE Int. Conf. Plasma Sci. 13th IEEE Int. Pulsed Power Conf.*, Jun. 2001, pp. 1245–1248.

[91] H. J. Ryoo, J. S. Kim, G. H. Rim, D. Sytykh, and G. Goussev, "Current loop gate driver circuit for pulsed power supply based on semiconductor switches," in *Proc. 16th IEEE Int. Pulsed Power Conf.*, Jun. 2007, p. 943.

[92] H. J. Ryoo, J. S. Kim, G. H. Rim, D. Sytykh, and G. Gussev, "Development of 60kV pulse power generator based on IGBT stacks for wide application," in *Proc. Conf. Rec. 27th Int. Power Modulator Symp.*, May 2006, pp. 511–514.

[93] H. J. Ryoo, G. Gussev, and S. R. Jang, "Development of 10kV, 50A, 50 kHz high repetitive pulsed power modulator based on IGBT stacks," in *Proc. IEEE Int. Power Modulators High-Voltage Conf.*, May 2008, pp. 384–387.

[94] S. Jang, H. Ryoo, and G. Goussev, "Compact and high repetitive pulsed power modulator based on semiconductor switches," *IEEE Trans. Dielectr. Electr. Insul.*, vol. 18, no. 4, pp. 1242–1249, Aug. 2011.

[95] C.-H. Yu, S.-R. Jang, H.-S. Kim, and H.-J. Ryoo, "Gate driving circuit with active pull-down function for a solid-state pulsed power modulator," *IEEE Trans. Power Electron.*, vol. 33, no. 1, pp. 240–247, Jan. 2018.

[96] E. H. W. M. Smulders, B. E. J. M. Van Heesch, and S. S. V. B. van Paasen, "Pulsed power corona discharges for air pollution control," *IEEE Trans. Plasma Sci.*, vol. 26, no. 5, pp. 1476–1484, Oct. 1998.

[97] J. Pelletier and A. Anders, "Plasma-based ion implantation and deposition: A review of physics, technology, and applications," *IEEE Trans. Plasma Sci.*, vol. 33, no. 6, pp. 1944–1959, Dec. 2005.

[98] S. Liu and M. Neiger, "Excitation of dielectric barrier discharges by unipolar submicrosecond square pulses," *J. Phys. D: Appl. Phys.*, vol. 34, no. 11, p. 1632, 2001.

[99] J. M. Williamson, "Comparison of high-voltage ac and pulsed operation of a surface dielectric barrier discharge," *J. Phys. D: Appl. Phys.*, vol. 39, no. 20, p. 4400, 2006.

[100] A. Meriched, M. Féliachi, and H. Mohellebi, "Electromagnetic forming of thin metal sheets," *IEEE Trans. Mag.*, vol. 36, no. 4, pp. 1808–1811, Jul. 2000.

[101] L. M. Redondo, J. Fernando Silva, and E. Margato, "Analysis of a modular generator for high-voltage, high-frequency pulsed applications, using low voltage semiconductors (<1kV) and series connected step-up (1:10) transformers," *Rev. Sci. Instrum.*, vol. 78, no. 3, Mar. 2007, Art. no. 034702.

[102] T. Jorge, M. T. Pereira, and L. M. Redondo, "New solid-state modulator for magnetic forming with energy recovering," in *Proc. 19th IEEE Pulsed Power Conf. (PPC)*, Jun. 2013, pp. 1–5.

[103] L. M. Redondo, T. Jorge, and M. T. Pereira, "Modular high-current generator for electromagnetic forming with energy recovery," *IEEE Trans. Plasma Sci.*, vol. 42, no. 10, pp. 3043–3047, Oct. 2014.

[104] H. Canacsinh and J. F. L. M. S. Redondo, "Rise-time improvement in bipolar pulse solid-state Marx modulators," *IEEE Trans. Plasma Sci.*, vol. 45, no. 10, pp. 2656–2660, Oct. 2017.

[105] H. Canacsinh, J. F. Silva, and L. M. Redondo, "Dual resonant voltage droop compensation for bipolar solid-state Marx generator topologies," *IEEE Trans. Plasma Sci.*, vol. 47, no. 1, pp. 1017–1023, Jan. 2019.

[106] G. E. Leyh, "Development and testing of the ILC Marx modulator," in *Proc. IEEE Part. Accel. Conf. (PAC)*, Jun. 2007, pp. 849–851.

[107] T. Tang, C. Burkhart, and M. Nguyen, "A Vernier regulator for ILC Marx droop compensation," in *Proc. IEEE Pulsed Power Conf.*, Jun. 2009, pp. 1402–1405.

[108] R. L. Cassel, "Pulsed voltage droop compensation for solid state Marx modulator," in *Proc. IEEE Int. Power Modulators High-Voltage Conf.*, May 2008, pp. 117–119.

[109] H. Canacsinh, "Solid-state bipolar Marx generator with voltage droop compensation," in *Proc. Technol. Innov. Value Creation 3rd IFIP WG 5.5/SOCOLNET Doctoral Conf. Comput., Elect. Ind. Syst. (DoCEIS)*, Costa de Caparica, Portugal, Feb. 2012, pp. 411–418.

[110] H. Canacsinh, L. M. Redondo, J. F. Silva, and B. Borges, "Voltage droop compensation based on resonant circuit for generalized high voltage solid-state Marx modulator," in *Proc. IEEE Appl. Power Electron. Conf. Expo. (APEC)*, Mar. 2016, pp. 3637–3640.

[111] H. Canacsinh, F. A. Silva, L. M. Redondo, and P. Botelho, "Increasing the voltage droop compensation range in generalized bipolar solid-state Marx modulador," in *Proc. IEEE 21st Int. Conf. Pulsed Power (PPC)*, Jun. 2017, pp. 1–4.

[112] H. Canacsinh *et al.*, "Optimized solid-state bipolar Marx modulador with resonant type droop compensation," in *Proc. IEEE 21st Int. Conf. Pulsed Power (PPC)*, Jun. 2017, pp. 1–4.

[113] H. Canacsinh and J. F. L. M. S. Redondo, "PWM voltage droop compensation for bipolar solid-state Marx generator topologies," *IEEE Trans. Plasma Sci.*, vol. 45, no. 6, pp. 975–980, Apr. 2017.

[114] L. Encarnao, "A new modular Marx derived multilevel converter," in *Proc. Technol. Innov. Sustainability 2nd IFIP WG 5.5/SOCOLNET Doctoral Conf. Comput., Elect. Ind. Syst., (DoCEIS)*, Costa de Caparica, Portugal, Feb. 2011, pp. 573–580.

[115] L. L. Rocha and J. F. L. M. S. Redondo, "Seven-level unipolar/bipolar pulsed power generator," *IEEE Trans. Plasma Sci.*, vol. 44, no. 10, pp. 2060–2064, Oct. 2016.

[116] I. Abdelsalam, M. A. Elgenedy, S. Ahmed, and B. W. Williams, "Full-bridge modular multilevel submodule-based high-voltage bipolar pulse generator with low-voltage DC, input for pulsed electric field applications," *IEEE Trans. Plasma Sci.*, vol. 45, no. 10, pp. 2857–2864, Oct. 2017.

[117] S. Jiang, L. Qiu, Z. Li, L. Zhang, and J. Rao, "A new all-solid-state bipolar high-voltage multilevel generator for dielectric barrier discharge," *IEEE Trans. Plasma Sci.*, vol. 48, no. 4, pp. 1076–1081, Apr. 2020.

[118] L. L. Rocha, J. F. Silva, and L. M. Redondo, "Marx multilevel bipolar modulator dynamic models for load transient analysis," *IEEE Trans. Plasma Sci.*, vol. 45, no. 10, pp. 2611–2617, Oct. 2017.

[119] M. A. Elgenedy, "A modular multilevel-based high-voltage pulse generator for water disinfection applications," *IEEE Trans. Plasma Sci.*, vol. 44, no. 11, pp. 2893–2900, Nov. 2016.

[120] M. A. Elgenedy, A. Darwish, S. Ahmed, and B. W. Williams, "A transition arm modular multilevel universal pulse-waveform generator for electroporation applications," *IEEE Trans. Power Electron.*, vol. 32, no. 12, pp. 8979–8991, Dec. 2017.

[121] M. A. Elgenedy, A. M. Massoud, S. Ahmed, B. W. Williams, and J. R. McDonald, "A modular multilevel voltage-boosting Marx pulse-waveform generator for electroporation applications," *IEEE Trans. Power Electron.*, vol. 34, no. 11, pp. 10575–10589, Nov. 2019.

[122] Z. Zeng, "On-off behavior control of SiC MOSFET by gate drive loops," *Zhongguo Dianji Gongcheng Xuebao/Proc. Chin. Soc. Elect. Eng.*, vol. 38, no. 4, pp. 1165–1176, 2018.

[123] Y. Mi, H. Wan, C. Bian, W. Peng, and L. Gui, "An MMC-based modular unipolar/bipolar high-voltage nanosecond pulse generator with adjustable rise/fall time," *IEEE Trans. Dielectr. Electr. Insul.*, vol. 26, no. 2, pp. 515–522, Apr. 2019.

[124] Y. Liu, R. Fan, X. Zhang, Z. Tu, and J. Zhang, "Bipolar high voltage pulse generator without H-bridge based on cascade of positive and negative Marx generators," *IEEE Trans. Dielectr. Electr. Insul.*, vol. 26, no. 2, pp. 476–483, Apr. 2019.

[125] M. Zarghani and S. S. M. Kaboli, "A high voltage pulsed power supply with online rise time adjusting capability for vacuum tubes," *IEEE J. Emerg. Sel. Topics Power Electron.*, vol. 9, no. 3, pp. 3019–3029, Jun. 2020.

[126] J. F. Rao, Z. Li, K. Xia, and S. Xin, "An all solid-state repetitive high-voltage rectangular pulse generator based on magnetic switch," *IEEE Trans. Dielectr. Electr. Insul.*, vol. 22, no. 4, pp. 1976–1982, Aug. 2015.

[127] L. Kefu, "Research progress of solid-state Marx generator," *High Voltage Technol.*, vol. 41, no. 6, pp. 1781–1787, 2015.

[128] W. Ding, H. Ren, Q. Zhang, and L. Yang, "Repetitive frequency Marx generator based on magnetic switches and its application in dielectric barrier discharge," *IEEE Trans. Plasma Sci.*, vol. 40, no. 10, pp. 2373–2378, Oct. 2012.

[129] D. Wang, J. Qiu, and K. Liu, "All-solid-state repetitive pulsed-power generator using IGBT and magnetic compression switches," *IEEE Trans. Plasma Sci.*, vol. 38, no. 10, pp. 2633–2638, Oct. 2010.

[130] D. Wang, J. Qiu, and K. Liu, "All solid-state pulsed power generator with semiconductor and magnetic compression switches," in *Proc. IEEE Pulsed Power Conf.*, Jun. 2009, pp. 1233–1238.

[131] J. N. Nasab, A. Hadizade, S. Mohsenzade, M. Zarghany, and S. Kaboli, "A Marx-based generator with adjustable FWHM using a controllable magnetic switch," *IEEE Trans. Dielectr. Electr. Insul.*, vol. 26, no. 2, pp. 324–331, Apr. 2019.

[132] L. Pang, T. Long, K. He, Y. Huang, and Q. Zhang, "A compact series-connected SiC MOSFETs module and its application in high voltage nanosecond pulse generator," *IEEE Trans. Ind. Electron.*, vol. 66, no. 12, pp. 9238–9247, Dec. 2019.

[133] W. Zeng *et al.*, "Self-triggering high-frequency nanosecond pulse generator," *IEEE Trans. Power Electron.*, vol. 35, no. 8, pp. 8002–8012, Aug. 2020.

[134] R. Junfeng, L. Encheng, W. Yonggang, J. Song, and L. Zi, "Self-triggering all-solid-state Marx generator," *High Power Laser Part. Beams*, vol. 33, no. 2, pp. 025001-1–025001-6, Jun. 2021.

[135] W. Jiang, T. Matsuda, K. Yatsui, and A. Tokuchi, "MHz pulsed power generator using MOSFET," in *Proc. Conf. Rec. 25h Int. Power Modulator Symp., High-Voltage Workshop.*, 2002, pp. 599–601.

[136] S. Jiang, "Design of MHz high voltage pulse power supply," *High Power Laser Part. Beams*, vol. 31, no. 9, 2019, Art. no. 095001.

[137] F. Pereira, L. Gomes, and L. Redondo, "FPGA controller for power converters with integrated oscilloscope and graphical user interface," in *Proc. Int. Conf. Power Eng., Energy Electr. Drives*, May 2011, pp. 1–6.
[138] F. Pereira, L. Gomes, and L. M. Redondo, "Multifunctional controller architecture for solid-state Marx modulator based on FPGA," *IEEE Trans. Plasma Sci.*, vol. 42, no. 10, pp. 2991–2997, Oct. 2014.
[139] Z. Li, H. Liu, S. Jiang, and J. Rao, "A novel drive circuit with overcurrent protection for solid state pulse generators," *IEEE Trans. Dielectr. Electr. Insul.*, vol. 26, no. 2, pp. 361–366, Apr. 2019.
[140] J. Rao, T. Zeng, S. Jiang, K. Xia, and Z. Li, "Synchronous drive circuit with current limitation for solid-state pulsed power modulators," *IET Power Electron.*, vol. 13, no. 1, pp. 60–67, Jan. 2020.
[141] L. Redondo, H. Canacsinh, and J. Silva, "New technique for uniform voltage sharing in series stacked semiconductors," *IEEE Trans. Dielectr. Electr. Insul.*, vol. 18, no. 4, pp. 1130–1136, Aug. 2011.
[142] Y. Wang, K. Liu, J. Qiu, and W. Dong, "A stage-stage paralleled topology of all-solid-state Marx generator for high current," *IEEE Trans. Plasma Sci.*, vol. 47, no. 10, pp. 4488–4494, Oct. 2019.
[143] Y. He *et al.*, "A polarity-adjustable nanosecond pulse generator suitable for high impedance load," IEEE Transactions on Plasma Science, vol. 48, no. 10, pp. 3409–3417, Oct. 2020.

Zhengyi Zhong was born in Sichuan, China, in 1997. He received the B.S. degree in electrical engineering from Shanghai Dianji University, Shanghai, China, in 2019. He is currently pursuing the Ph.D. degree in pulsed power technology with the University of Shanghai for Science and Technology, Shanghai.

Junfeng Rao (Senior Member, IEEE) was born in Xianning, Hubei, China, in 1985. He received the B.Eng. degree in electrical engineering from the Huazhong University of Science and Technology, Wuhan, China, in 2008, and the Ph.D. degree from Fudan University, Shanghai, China, in 2013.

He is currently an Associate Professor with the University of Shanghai for Science and Technology, Shanghai. His research interests include pulsed power technology and applications.

Haotian Liu was born in Tangshan, Hebei, China, in 1995. He received the B.Eng. and M.Sc. degrees in electrical engineering from the University of Shanghai for Science and Technology, Shanghai, China, in 2017 and 2020, respectively. He is currently pursuing the Ph.D. degree in pulsed power technology with Fudan University, Shanghai.

L. M. Redondo (Senior Member, IEEE) received the B.Sc. and Dipl.Eng. degrees in electrical engineering from ISEL-IPL, Lisbon, Portugal, in 1990 and 1992, respectively, the M.Sc. degree in nuclear physics from FCUL, Lisbon, in 1996, and the Ph.D. degree in electrical and computer engineering from IST-UTL, Lisbon, in 2004.

He is currently a Coordinate Professor with ISEL, teaching power electronics and digital systems. In 2011, he founded Energy Pulse Systems, Lisbon, where he is a Technology Manager. In 2015, he founded the Association for the Advancement of Pulsed Power, Lisbon, where is he currently the Vice-President. His research interest includes pulsed power systems for industrial applications.

Dr. Redondo was an Elected Voting Member of the Pulsed Power Science and Technology Committee from NPSS/IEEE in 2020, for a 3-year period.